Electrophysiological Studies of the Feasibility of Suprachoroidal-Transretinal Stimulation for Artificial Vision in Normal and RCS Rats

Hiroyuki Kanda,[1,2,3] *Takeshi Morimoto,*[1,2,4] *Takashi Fujikado,*[2,4] *Yasuo Tano,*[4] *Yutaka Fukuda,*[1] *and Hajime Sawai*[1]

PURPOSE. Assessment of a novel method of retinal stimulation, known as suprachoroidal-transretinal stimulation (STS), which was designed to minimize insult to the retina by implantation of stimulating electrodes for artificial vision.

METHODS. In 17 normal hooded rats and 12 Royal College of Surgeons (RCS) rats, a small area of the retina was focally stimulated with electric currents through an anode placed on the fenestrated sclera and a cathode inserted into the vitreous chamber. Evoked potentials (EPs) in response to STS were recorded from the surface of the superior colliculus (SC) with a silver-ball electrode, and their physiological properties and localization were studied.

RESULTS. In both normal and RCS rats, STS elicited triphasic EPs that were vastly diminished by changing polarity of stimulating electrodes and abolished by transecting the optic nerve. The threshold intensity (C) of the EP response to STS was approximately 7.2 ± 2.8 nC in normal and 12.9 ± 7.7 nC in RCS rats. The responses to minimal STS were localized in an area on the SC surface measuring 0.12 ± 0.07 mm^2 in normal rats and 0.24 ± 0.12 mm^2 in RCS rats. The responsive area corresponded retinotopically to the retinal region immediately beneath the anodic stimulating electrode.

CONCLUSIONS. STS is less invasive in the retina than stimulation through epiretinal or subretinal implants. STS can generate focal excitation in retinal ganglion cells in normal animals and in those with degenerated photoreceptors, which suggests that this method of retinal stimulation is suitable for artificial vision. (*Invest Ophthalmol Vis Sci.* 2004;45:560-566) DOI:10.1167/iovs.02-1268

Since it was first proposed by Tassicker in 1956,[1] a retinal prosthesis for artificial vision has remained conceptual. During the past decade, however, a retinal prosthesis has become much more realistic and has been supported by recent developments of implantable materials and microelectronics (see reviews[2-5]). Previous in vivo experiments have indicated that impaired parts of the retinal network can be bypassed by electrical stimulation to the retina by microelectrode arrays implanted in the eye.[6-10] Results obtained in animal experiments suggest that retinal implantation of stimulating devices hold great promise for restoration of the vision of people with outer retinal degeneration, such as retinitis pigmentosa (RP) and age-related macular degeneration (AMD). Although there have been a few optimistic reports of retinal implants for human patients,[11-13] there is room for improvement of electrode arrays for clinical application.

Two ways of stimulating the retina for artificial vision are currently well developed. One is subretinal stimulation (SRS), in which a sheet containing a microphotodiode array is inserted into the subretinal space to compensate for lost photoreceptor function and stimulate the outer retinal network.[6,7,14] The other is epiretinal stimulation (ERS), in which retinal ganglion cells (RGCs) and their axons are stimulated with a multielectrode array attached to the vitreous side of the retina.[8-13] Either type of retinal stimulation has its own advantages and disadvantages.[3] For example, fixing the electrode array is easier with SRS than ERS. In contrast, SRS requires intact optics, whereas ERS does not, and SRS needs a great deal more electrical power than does ERS. Whereas SRS can use retinal circuitry, ERS requires the processing of visual information into specific patterns for the stimulation of RGCs. One common drawback of both types of implants is that implanted electrodes are directly attached to the retina, so that the risk of retinal damage at implantation is inevitable. Although some reports claim that there is no detectable damage to the retina after long-term implantation of microelectrode arrays,[14-16] surgical difficulties remain if removal or replacement is necessary, both of which are possible. From a clinical viewpoint, it is therefore preferable to have the stimulating electrodes of implants placed away from the retina.

To meet this clinical need, we designed a novel type of transretinal stimulation, with electrodes unattached to the retina. We named it "suprachoroidal-transretinal stimulation" (STS), in which the anodic stimulating electrode is positioned on the choroidal membrane and the cathode is placed in the vitreous body. Because it has been demonstrated that various types of transretinal stimulation can induce field responses in central visual areas,[17,18,19,20] STS can be expected to activate the retinal network. Our major concern regarding STS is that, because the suprachoroidally placed electrodes are not in contact with the retina, the following disadvantages for artificial vision may result. First, STS may be much less effective than ERS and SRS, resulting in a high threshold for stimulation of the retinal circuitry. The strong electrical stimulation of STS may damage the retina and increase the power load on implanted electronic devices. Second, STS may stimulate a much broader area of the retina than SRS and ERS do, resulting in such a low resolution that artificial vision is impossible.

To test the feasibility of STS for artificial vision, we addressed a critical question in the study reported herein—namely, whether local application of STS can evoke definite responses in the primary visual center that receives direct input from the retina. If this is the case, the localization and threshold of the evoked response are also important issues to

From the Departments of [1]Physiology and Biosignaling, [2]Visual Science, and [4]Ophthalmology, Graduate School of Medicine, Osaka University, Suita, Japan; and [3]Nidek Co., Ltd., Gamagouri, Japan.

Supported by Health Sciences Research Grants from the Ministry of Health, Labor and Welfare, and the New Energy and Industrial Technology Development Organization (NEDO), Japan.

Submitted for publication December 11, 2002; revised July 19 and September 22, 2003; accepted October 29, 2003.

Disclosure: **H. Kanda**, None; **T. Morimoto**, None; **T. Fujikado**, None; **Y. Tano**, None; **Y. Fukuda**, None; **H. Sawai**, None

The publication costs of this article were defrayed in part by page charge payment. This article must therefore be marked "*advertisement*" in accordance with 18 U.S.C. §1734 solely to indicate this fact.

Corresponding author: Hajime Sawai, Department of Physiology and Biosignaling, Graduate School of Medicine, Osaka University, 2-2 Yamadaoka, Suita, Osaka 565-0871, Japan; h_sawai@phys2.med.osaka-u.ac.jp.

Investigative Ophthalmology & Visual Science, February 2004, Vol. 45, No. 2
Copyright © Association for Research in Vision and Ophthalmology

examine. To answer this question, we performed acute electrophysiological experiments using the rat retinocollicular system. The superior colliculus (SC) in rats is easily accessible for recording responses to retinal stimulation. Because of the precise retinotopic organization of the SC,[21] localization of the collicular response could tell us the extent of the retinal area stimulated by STS. From a clinical perspective for further development of STS for human RP, we used Royal College of Surgeons (RCS) rats and normal hooded rats. RCS rats, with inherited retinal degeneration that seems to resemble human RP,[22] are well established as one of the best animal models for retinal degeneration.[23] With this retinal dystrophic rat we were able to investigate whether STS can stimulate the residual circuitry of the inner retina and can be used for artificial vision in human RP.

Methods

Animals

As experimental animals, male hooded rats (Long-Evans; SLC Japan Inc., Hamamatsu, Japan; $n = 17$) from 8 to 14 weeks old and RCS rats (inbred at the Department of Ophthalmology, Osaka University; $n = 12$) from 25 to 30 weeks old were used. All animals were housed under a 12-hour light-dark cycle. All procedures conformed to the ARVO Statement for the Use of Animals in Ophthalmic and Vision Research. Every effort was made to minimize animal discomfort and to use only the number of animals necessary to produce reliable scientific data.

Surgical Preparation

The animals were anesthetized initially with urethane (1.75 g/kg, intraperitoneally). The same anesthetic was administered (0.5 g/kg, intraperitoneally) every 3 hours to keep them anesthetized during the surgical preparations and electrophysiological experiments. A heating pad was used to maintain body temperature at approximately 37°C. Heart rate and electrocardiogram (ECG) were monitored throughout the experiments. The pupils were dilated with a mydriatic (Midorin P; Santen Pharmaceutical Co., Ltd., Osaka, Japan), and the corneas were covered with contact lenses.

After tracheal cannulation, the heads of the animals were fixed stereotaxically. Cerebrospinal fluid was drained through a small incision made into the dura on the obex. Craniotomy was performed on the right side of the temporal bone, and the underlying occipital cortex was removed by gentle aspiration to expose the dorsal surface of the SC. The surface of the SC was filled with mineral oil during the experiments to prevent drying and leakage of current from the recording electrodes. For stimulation of the retina or the optic nerve (ON), the sclera and the ON of the left eye were exposed intraorbitally. After incision of the surrounding tissue and the dura mater, the ON was exposed very carefully to avoid retinal ischemia.

Photic and Electrical Stimulation

The light source, a photic and sonic stimulator (Nihon Kohden, Tokyo, Japan), was positioned 5 cm in front of the left eye. Stimuli consisting of single flashes were given at intervals of 3 to 5 seconds, and electroretinogram (ERG) or collicular EP was recorded.

For electrical stimulation, a silver-ball-stimulating electrode (suprachoroidal electrode or S-electrode, diameter: 0.2-0.3 mm) was inserted into a small lamellar scleral resection (diameter: approximately 0.5 mm) made at a distance of 1.5 to 2.5 mm from the ON in the upper temporal part of the sclera. The stimulating electrode, electrically isolated from the surrounding tissue with mineral oil, was used as an anode. A cathodic electrode of epoxy-coated stainless wire (vitreous body electrode or V-electrode, diameter: 0.2 mm) with approximately 2 mm of the tip exposed was inserted approximately 4 mm into the vitreous. A single monophasic pulse of electrical current was applied between these two electrodes through an isolator (SS-202J; Nihon Kohden, Tokyo, Japan) connected to an electrical stimulator (SEN-7203; Nihon Kohden) for 0.05, 0.2, or 0.5 ms, depending on the level of the EP threshold. The range of current amplitude was 5 to 300 μA. Inward stimulation between the anodic S-electrode and the cathodic V-electrode was used as the standard, and outward stimulation was tested when necessary. The ON was also stimulated with a pair of silver-ball electrodes placed in the intraorbital section, approximately 3 mm behind the globe.

Electrophysiological Recordings

A silver-ball recording electrode (Ag/AgCl, 0.2-0.3 mm in diameter) was moved systematically by means of a hydraulic three-dimensional micromanipulator (MMW; Narishige Science Institute Laboratory, Tokyo, Japan) and placed on the exposed SC surface. A stainless-steel screw was implanted into the occipital bone approximately 1 mm behind the lambda and used as a reference electrode. Responses from the SC were amplified 10,000 times with a band-pass of 15 Hz to 3 kHz. Approximately 50 evoked responses were averaged with a signal processor (LEG-1000; Nihon Kohden).

A flash ERG was also recorded from the left eye using a contact lens electrode (Kyoto Contact Lens, Kyoto, Japan) after a 20-minute scotopic adaptation. ERG responses were amplified 10,000 times with a band-pass of 1 Hz to 3 kHz.

Histologic Analysis

After electrophysiological recordings were obtained from the right SC, a small incision was made with a fine needle at the site where the largest EPs were recorded, as a reference point for reconstruction of the recording sites on the SC. A suture was made at the dorsal pole of the stimulated eye as a marker for retinal orientation. The animals were then deeply anesthetized with a lethal dose of pentobarbitone sodium and perfused intracardially with 0.1 M phosphate-buffered saline (PBS) followed by a fixative (4% paraformaldehyde in PBS). The fixed eye and midbrain were resected for histologic examination under a binocular microscope.

The distance was measured between the optic disc and the position of the S-electrode, which was easily identified by the resection scar on the sclera, and no adjustment was made for shrinkage after fixation. Micrographs of the posterior view of the eye with the optic nerve head, the scar, and the suture at the dorsal pole were taken with a digital camera attached to the microscope. Micrographs were also taken of the dorsal view of the midbrain for reconstruction of the recording sites. Because of shrinkage of the midbrain after fixation, the digital images were sufficiently enlarged that reference incisions for recording sites could be adjusted with their stereotaxic coordinates. The outlines of the SC and the recording sites were then extracted from these adjusted images.

After identification of the position of the stimulating electrode, the eyes were hemisected to make eye cups, which were postfixed and then cryoprotected with 25% sucrose in PBS. Vertical cryosections of the retinal cups were made by means of a freezing microtome (CM1900; Leica, Solms, Germany). These sections were then mounted on gelatinized glass slides and stained with hematoxylin and eosin. Finally, the stained specimens were dehydrated, cleared, and coverslipped for microscopic analysis of the cytoarchitecture of the retinas.

Results

Field Responses to STS in Normal Hooded Rats

We examined first whether focal STS evokes collicular responses. With a brief pulse of a constant current (0.5 ms, 100 μA) applied transretinally, evoked potentials (EPs) were consistently obtained from the contralateral SC. Because the amplitudes of the responses depended on the recording site within the SC and the intensity of the current, we first identified the center of the responsive area (CRA) where the largest EPs were recorded for a given intensity of STS. Next, the

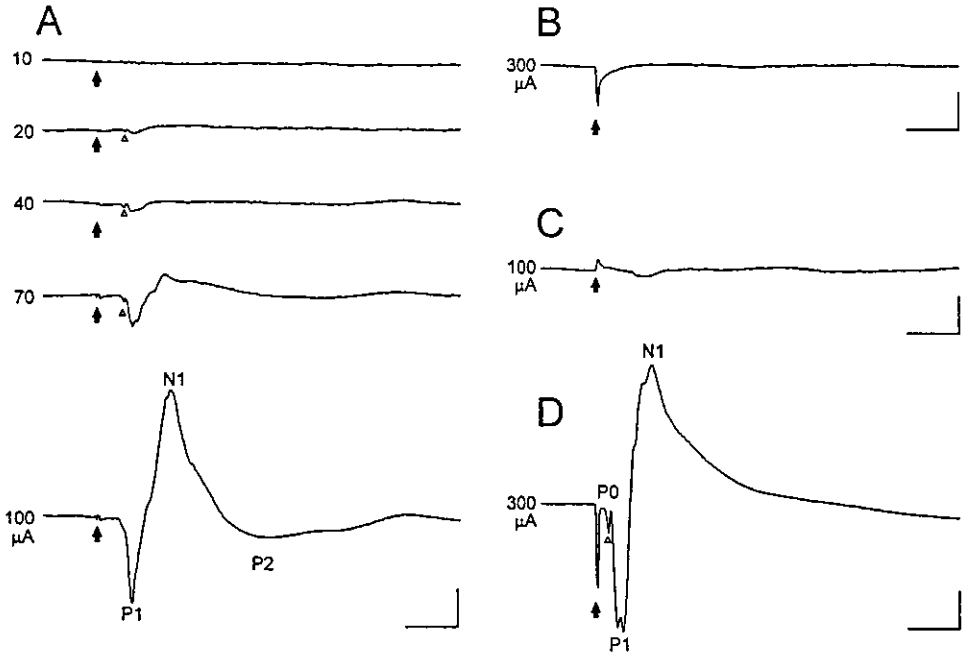

FIGURE 1. EPs recorded from the SC to inward STS (A, B), outward STS (C) and ON stimulation (D) in a hooded rat. Stimulus intensity (in microamps) is indicated at the *left* of each trace. (A) The EPs consisted of a fast positive wave and a slow negative potential (N1) with a P0 (△) that was identified in the second to the fourth trace. The threshold currents for the activation of P1 were 10 to 20 μA. (B) The EPs to STS disappeared after the ON was severed. (C) In outward STS, the amplitude of EPs decreased. (D) The EPs to the ON also consisted of P0, P1, and P2. *Arrows*: onset of stimulus. Calibration: (A, B, C) 50 μV, 10 ms; (D) 100 μV, 10 ms.

stimulus intensity dependence of the EPs at CRA was examined.

Figure 1A shows a typical series of EPs at the CRA for various intensities of stimulation in a normal hooded rat. With suprathreshold level of STS, the EPs were composed of a sharp positive deflection (P1) followed by a large negative wave (N1) and a small, long-lasting positive wave (P2). The N1 wave was occasionally accompanied by another small negative deflection (N2; see Figs. 2E, 2F). The ranges of the peak latencies of the P1, N1, and P2 components were 6.7 ± 1.1 ms (mean ± SD; $n = 14$), 15.3 ± 4.3 ms ($n = 14$), and 34.6 ± 6.5 ms ($n = 10$), respectively. The amplitude of these three components was reduced by tetanus stimulation (at a frequency of approximately 50 Hz), indicating that these responses were postsynaptic (data not shown). At a medium intensity of stimulation (20–80 μA, 0.5 ms: 10–40 nC), a small positive wave (P0) was

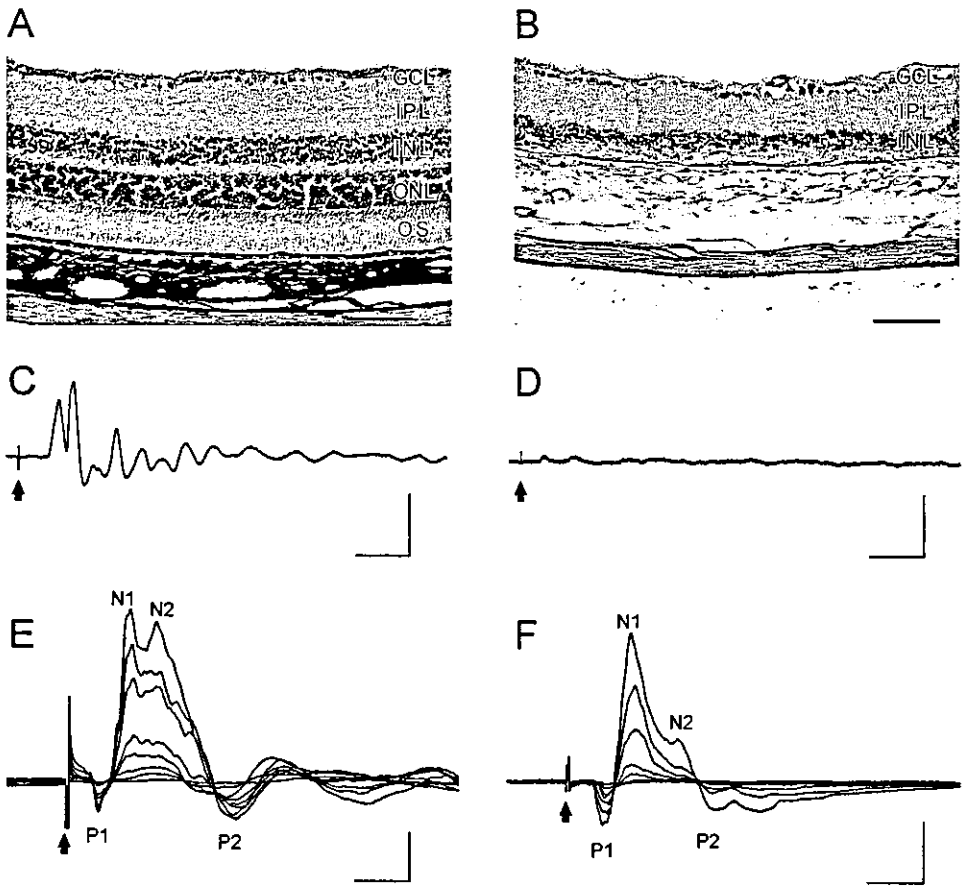

FIGURE 2. Comparison of retinal cytoarchitecture and collicular EPs of hooded and RCS rats. Photomicrographs of hematoxylin-eosin-stained retinal sections of hooded (A) and RCS rats (B) show complete loss of the outer retinal layers in the RCS rat. Flashing-light stimuli generated EPs from the SC of hooded (C) but not RCS (D) rats. The inward STS generated EPs from both hooded (E) and RCS (F) rats. OS, outer segment; ONL, outer nuclear layer; INL, inner nuclear layer; IPL, inner plexiform layer; GCL, ganglion cell layer. Stimulus intensities were 10, 30, 50, 80, 100, 150, 200, and 300 μA in (E) and 30, 50, 80, 100, 150, 200, and 300 μA in (F). *Arrows*: onset of stimulus. Calibration: (C, D) 100 μV, 50 ms; (E, F) 100 μV; 10 ms. Scale bar: (A, B) 100 μm.

often recorded before the P1 wave at a peak latency of 4 to 5 ms, with a peak amplitude of 2 to 10 μV (Fig. 1A; small open triangle). At higher intensities of stimulation, P0 was engulfed by P1 and remained as a notch in the rising phase of the P1 wave. The amplitude did not change with high-frequency stimulations (up to 100 Hz), indicating that the wave reflects the responses of the retinal axon terminals.[24] At lower stimulus intensities, the EPs became smaller, and only P0 and P1 remained at 20 μA (10 nC), whereas no response was observed below 10 μA (5 nC). The mean (±SD) threshold of STS for evoking EPs was 7.2 ± 2.8 nC (n = 6). The EPs were completely abolished after transection of the ON just behind the eyeball (Fig. 1B). Thus, it is unlikely that retinal stimulation directly stimulated the ON and/or the SC.

The threshold of the EPs also depended on the polarity of stimulation. When the stimulating current passed from the V-electrode to the S-electrode (outward stimulation through the retinas), the threshold of the EP dramatically increased from 10 to 60 μA, and, even at 100 μA, only a small P1 was observed (Fig. 1C). In all six cases we examined, switching to outward STS reduced the P1 to N1 amplitude to an average of one tenth. Moreover, this change in stimulus polarity slightly prolonged the peak latency of EPs in two thirds of the examinations. Figure 1C shows the extension of the P1 latency from 7.0 to 9.5 ms.

Field Responses to ON Stimulation in Normal Hooded Rats

To determine whether STS directly activates the ON, we electrically stimulated the ON to record EPs from the CRA of the SC, and compared these EPs with those in response to the retinal stimulation. The EPs for the supramaximal ON stimulation consisted of two positive deflections (P0, P1) followed by a negative deflection (N1), as shown in Figure 1D. The first positive deflection (P0) and the other two components (P1, N1) were identified as presynaptic (ON fiber terminals-derived) and postsynaptic, respectively, because P1and N1 were completely eliminated by tetanic stimulation, but P0 was unaffected.[24] These three components corresponded well to T1, C1, and C2, as designated by Sefton in 1969.[25] The mean peak latencies of these components (P0, P1, and N1) were 2.5 ± 0.1, 4.3 ± 0.4, and 9.5 ± 0.5 ms, respectively, thus consistently shorter than those of the EPs elicited by the retinal stimulation (P1: P = 0.029, N1: P = 0.035, Student's paired t-test). The statistically significant differences in peak latency of EPs between STS and the ON stimulation rule out the possibility that STS stimulated the ON directly.

Field Responses to STS in RCS Rats

RCS rats have been used as one of the most effective animal models for human retinal dystrophy, especially RP.[23] To evaluate the suitability of an STS-based artificial retina for clinical application in patients with RP, we used RCS rats to investigate whether STS can bypass their degenerated outer retina and directly activate the residual retinal circuitry.

Figure 2 shows typical results for RCS rats. Histologic examination of RCS rats confirmed severe loss of the outer part of the retinas. The photoreceptor layer completely disappeared in an RCS rat (Fig. 2B) but not in a normal hooded rat (Fig. 2A). Although the inner nuclear layer of the RCS rat was slightly thinner than that of the normal hooded rat, cytoarchitecture of the inner half of the RCS retina seemed to be normal. Some cells with large somata, suggestive of RGCs, were identified in the ganglion cell layer. Moreover, immunostaining for PKC, known as a reliable marker of rod bipolar cells,[26] resulted in marked preservation of the bipolar cells in the inner nuclear layer of the RCS rats (data not shown).

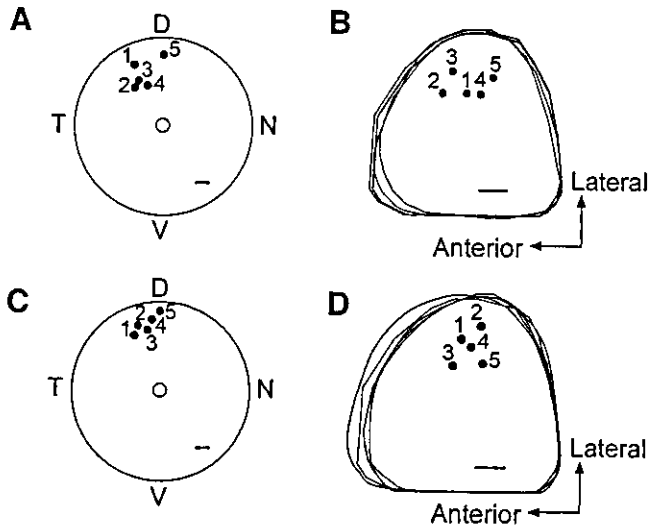

FIGURE 3. Topographic correspondence between the positions of the anodic S-electrodes (A: hooded, C: RCS) and the collicular sites (B: hooded, D: RCS) from which the maximum EPs were recorded in 10 representative animals. Individually numbered *filled* indicate the retinal positions of the S-electrodes. The corresponding sites with maximum EPs are plotted as *filled circles*. (A, C) Drawings of the posterior view of the eyes. The circle in the center is the ON. D, dorsal; N, nasal; T, temporal; V, ventral; (B, D) Drawings of the dorsal surface of the SC. Scale bars: (A, C) 1 mm; (B, D) 0.5 mm.

As could be expected from these results, neither ERG (data not shown) nor collicular EP (Fig. 2D) was recorded in response to the flashing-light stimulus in the RCS rat, whereas the same photic stimulus generated conspicuous EPs in the SC of the normal hooded rat (Fig. 2C). The STS (>20 μA for a 0.5-ms pulse) evoked clear field responses on the SC of the RCS rat (Fig. 2F). The EPs consisted of a fast positive wave (P1) followed by a slow negative wave (N1). The peak latencies of the P1 and the N1 were 7.1 ± 1.5 and 13.0 ± 2.8 ms, respectively (mean ± SD, n = 11). When electric current was increased up to 100 μA, the two peaks became very clear. The N1 was occasionally followed by a negative peak (N2) as seen in the case of the high-intensity stimulus. The mean ± SD of the N2 peak latency in normal hooded rats was 24.6 ± 4.8 (n = 7) and 25.6 ± 5.0 ms (n = 7) in RCS rats. The EPs to STS in the RCS rats were identical with those in the normal rats (Fig. 2E) in terms of shape an peak latencies of P0, N1 and P1, as well as threshold. The average threshold intensity of the EP in response to STS was approximately 12.9 ± 7.7 nC (n = 7) in RCS rats. It was slightly higher than that in normal hooded rats, but the difference was not statistically significant. The effect of changing the polarity of stimulating electrodes was confirmed in RCS rats. The amplitude of EPs decreased up to 8% by outward STS.

Topological Correspondence of Field Responses to the Retinal Stimulation Sites

Because it is well established that retinocollicular projections are topographically ordered,[21] the collicular positions of the CRA should correspond to the retinal regions in which RGC discharges were elicited by STS. To know whether RGCs below anodic S-electrodes were excited by STS, we examined topological relationship between positions of CRA in the SC and those of S-electrodes. Figure 3 illustrates the results obtained from five normal and five dystrophic rats. In Figures 3A and 3C, individually numbered dots indicate the position of the S-electrode at the dorsotemporal retina at a distance of 1.7 to 2.8 mm from the optic disc. The corresponding CRAs of these animals are plotted as numbered black dots in the outline of

their SCs as based on photographs of the midbrain after fixation (see the Methods section). In Figures 3B and 3D the drawings of these outlines have been placed on top of one other along the midline and posterior edge of the SC. The CRAs were consistently confined to the lateral part of the central SC, which is known to receive inputs exclusively from the upper retina (see Fig. 3 in Siminoff et al.[21]). Thus, there seems to be a topological relationship between the positions of the CRA and the S-electrodes, but not the V-electrodes.

Spatial Extent of Field Responses to the STS

To define the extent of the area that responded electrophysiologically to STS, the EPs were recorded at sites separated by 100 to 200 μm along the rostrocaudal and mediolateral axis of the SC. Because the extent of the responsive area varied with the intensity of STS, it was placed just above the threshold of the EPs at CRA. Figure 4 shows the smallest, intermediate, and largest areas responding to the minimum STS in normal (Fig. 4A) and dystrophic (Fig. 4B) rats . Filled circles indicate recording sites where an EP was obtained and are surrounded by unresponsive sites (horizontal bars). The smallest responsive area was less than a square with sides of 100 μm (Figs. 2, 4A), and the mean ± SE of the area was 0.12 ± 0.08 mm^2 (n = 5) in the normal rats. In dystrophic rats, the former was less than a square with sides of 200 μm (Figs. 3, 4B), and the latter area was 0.24 ± 0.12 mm^2 (n = 5). Thus, the method of retinal stimulation used in this study can excite a very small area of the SC, indicating that the retina is focally stimulated.

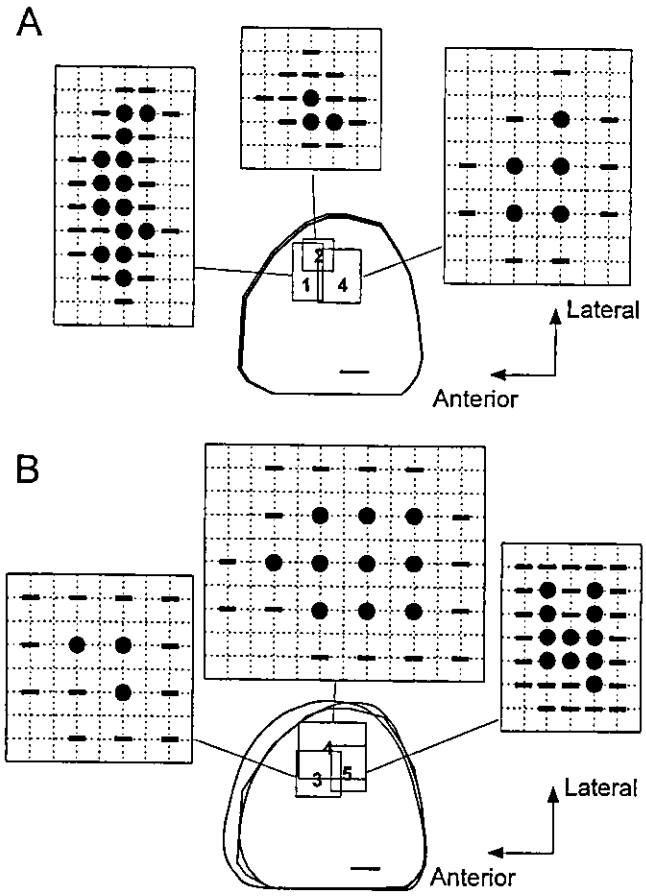

FIGURE 4. Localization of collicular EPs in response to a focal inward STS in hooded (A) and RCS (B) rats. The outlines of the SC surface of three animals were superimposed. The *numbers* in the squares correspond to those in Figure 3. In each of the *expanded squares*, the *filled circles* represent the sites where EPs were recorded, and the *horizontal bars* show the unresponsive sites. The intensities of STS were just above the threshold: 5 to 8 nC in hooded rats (A) and 10 to 30 nC in RCS rats (B). Scale bar: 0.5 mm; one grid interval, 100 μm.

Resolution of EP to STS at Two Separate Sites

Last, we investigated whether STS of two adjoining areas of the retina can evoke two discrete field responses in the SC of a normal hooded rat. A pair of S-electrodes, S1 and S2, were placed on the eyeball at a distance of approximately 0.7 mm from each other, and these two points were stimulated with an interval of 400 ms. The CRA to STS with the S1 electrode (STS1) was different from that with the S2 electrode (STS2). On the line between these two CRAs, EPs to STS1 and STS2 recorded at intervals of 0.1 mm showed a stimulus intensity of 52 nC (260 μA at a duration of 0.2 ms). Figure 5 illustrates the relative amplitudes of the EPs at each recording site, demonstrating that the response profile to STS1 was spatially differentiated by 0.5 to 0.6 mm from that to STS2. This means that spatial resolution of STS for artificial vision would be 0.7 mm at most.

Discussion

Several studies have demonstrated that ERS or SRS with microelectrode arrays elicits responses from visual centers.[6–10] In the present study, we developed a novel means of retinal stimulation for artificial vision (i.e., STS) and demonstrated that focal STS successfully produced localized excitation of the rat SC. This STS was applied through the anode on the fenestrated sclera and the cathode placed in the vitreous body, thus avoiding direct contact of stimulating devices with the retina. Localized EPs were recorded from a small and defined area of the contralateral SC, which corresponds retinotopically to the position of the anode. As with ERS and SRS it can thus be expected that spatially patterned STS through anodes arranged in an orderly manner on the sclera can provide visual centers with essential features of images on the retina.

Suitability of STS for Artificial Vision

By comparison with ERS and SRS, we assessed the suitability of STS for an artificial retina in terms of stimulus efficacy and spatial resolution. High efficacy of stimulation is very important in artificial vision because it results in localizing retinal excitation, preventing retinal damage from electricity, and reducing energy consumption. Efficacy of STS can be assessed by means of the threshold of the stimulation that elicits certain responses in visual centers. The threshold of the collicular response to STS in our study was as low as 5 to 8 nC. Although the threshold of STS is not as low as that of ERS or SRS (for example, 1–36 nC for SRS,[6] and 14 nC,[8] 0.1–0.3 nC,[9] or 0.5–6.0 nC[10] for ERS), it is still low enough for the design of an STS-based artificial retina. In fact, the threshold of STS was quite low when it is taken into account that neither of the stimulating electrodes was in contact with the retina. Probably because electrical resistance of the sclera is much higher than that of the retina and the vitreous, scleral fenestration under the anode may play a role in a highly conductive path, thus contributing to the reduction in the threshold of STS. In fact, we often found during preparation of the animals that the threshold of EPs to STS decreased by up to one half after the fenestration.

Another important question is how a localized area can be stimulated by STS, in that this is crucial for spatial resolution in artificial vision. With minimum stimulus intensity, the area where the EPs were recorded was limited to a few hundred square micrometers, which is roughly 2% of the whole surface area of the SC, or 6.4 mm^2. With this ratio, the area of the stimulated retina can be calculated as 1.1 mm^2, assuming that the whole retinal surface area is 57 mm^2 in rats,[27] and without

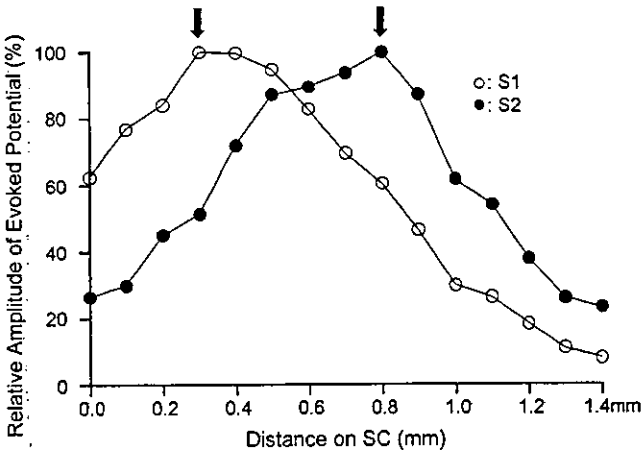

FIGURE 5. Spatial separation of amplitude profiles of EPs in response to inward STS between two different anodic electrodes, S1 (○) and S2 (●). Relative amplitudes of EPs are plotted on the ordinate and positions of the recording electrode on the abscissa. Distance between the two peaks on the surface of SC was 0.5 to 0.6 mm. *Arrows*: peak response sites to S1 and S2.

taking the retinocollicular magnification factor into consideration. Even such a rough estimation allows us to expect that a single STS to the human eye could activate approximately 1 mm^2 of the retina.

We also stimulated two retinal sites 700 μm apart, which resulted in discrimination of two different responsive areas in the SC. The distance of 700 μm on the human retina corresponds to a visual angle of approximately 2.4°.[28] Therefore, the estimated spatial resolution for STS-based artificial vision seems to be practical, although the resolution in STS is not as good as that for ERS or SRS, which is approximately 1°.[10] Downsizing the anode for STS may improve the spatial resolution.

Compared with ERS and SRS, STS has a major advantage for retinal prosthesis from the surgical point of view. For stimulation, an anodic microelectrode array can be implanted in the fenestrated sclera, and a cathode placed in the vitreous body. Thus, stimulating electrodes will never be in contact with the retina. This configuration of stimulating electrodes would be beneficial in terms of easier and less invasive implantation of the device into the retina. It would also make it easy to remove or replace the implants if necessary. The anodic electrode array would be placed in the intraorbital space, which is relatively large for the implantation of microdevices. This allows for easier design and manufacture of the array with fewer limitations of size and shape than for other implants directly attached to the retina, especially subretinal implants. With STS, moreover, many anodes could be independently implanted instead of a multiple electrode array, so that each of these anodes could be exchangeable individually.

STS in RCS Rats

STS is potentially suitable for retinal prostheses and artificial retinas. This conclusion is ultimately supported by the results obtained in RCS rats, a well-established model of human RP. To the best of our knowledge, this is the first study using RCS rats to demonstrate that localized electrical stimulation to the retina can bypass the degenerated outer retinal circuitry and provide excitation of the visual center, which receives inputs from RGCs.

The EPs to focal STS in the RCS rats were highly similar to those in the normal hooded rats in terms of waveform, peak latencies of the components, and threshold. This similarity suggests that the essential electrophysiological function of the inner retinal circuitry may be maintained even after the degeneration of photoreceptors. Histologic analysis proved that the organization of the inner nuclear layer, the inner plexiform layer, and the ganglion cell layer was normal, which agrees with previous findings that indicate that no transneuronal changes occur after the loss of photoreceptor cells.[29] On the contrary, there are reports of some abnormalities in horizontal, Müller, and bipolar cells.[30–33] Furthermore, it has been found in aged animals that secondary degeneration of RGCs occurs probably due to contraction of intraretinal vessels.[34] Feasibility of STS for artificial vision must therefore also be tested in aged RCS rats.

Preservation of normal retinofugal projection after the loss of photoreceptors is one of the prerequisites for an artificial retina. No information is available about the topographic organization of retinofugal projection in case of complete dysfunction of phototransduction, other than an anterograde tracing study that demonstrated that the projection patterns in RCS rats appeared similar to those in their congenic controls, although terminal density was somewhat reduced in dystrophic rats.[35] In the present study, EP-recording sites roughly showed topological correspondence to the retinal points stimulated at the anode in the RCS rats as well as in the normal rats. No significant difference was seen between the two strains in the extent of the retinal area activated by STS. These results do not necessarily imply, however, that the topological order of retinotectal projection survives in RCS rats after loss of photoreceptors. Further examination of this point is clearly needed.

Transretinally Stimulated Cells

What types of retinal neurons were stimulated by STS? Photoreceptor cells can be excluded because of our finding that STS evoked collicular responses, not only in normal hooded rats but also in RCS rats with degenerated photoreceptors. Exclusion of photoreceptors as a target of transretinal stimulation was also confirmed by Potts and Inoue,[18] who reported that a change in potential was recorded from the cortex of rats with hereditary photoreceptor degeneration on electrical stimulation applied to the globe. Other lines of evidence about electrically evoked potentials (EEPs) in response to various types of transretinal stimulation also indicate that photoreceptors are not involved in generation of the EEPs.[19,20,36] Therefore, STS must stimulate the inner retinal cells, such as bipolar cells, amacrine cells, and RGCs, to elicit collicular EPs.

According to electrophysiological principles, the inward transretinal current of STS has a depolarizing effect on the vitreous and a hyperpolarizing effect on the scleral side of every radially oriented retinal cell. Among the inner retinal cells, involvement of bipolar cells and their related synaptic sites in transretinal stimulation was indicated in a few reports using the intact retina.[20,36] Although the transretinal stimulation in these studies is different from STS, it is likely that STS could also stimulate bipolar cells and their related synaptic sites. The possibility of the RGC as a target for stimulation was excluded by the authors in those studies.[18,19,36] For example, Stett et al.[36] demonstrated in vitro that ganglion cell discharge in response to transretinal stimulation in the chick retina was reduced or eliminated after the application of agents for blocking synaptic transmission. However, when nine neighboring points were stimulated simultaneously (so-called box stimulation), the fast spike and delayed response remained, even after application of a perfusate with a high concentration of Mg^{2+}, which suggests that direct stimulation of RGCs may occur when the stimulated area extends within a square with sides of 200 μm. Because this size is comparable to that of the fenestrated area used in our study, it is possible that STS stimulates RGCs directly. Moreover, using isolated frog retinas, Li et al. have provided evidence of direct excitation of RGCs by transretinal stimulation (Li, et al. *IOVS* 2002;43:ARVO E-Abstract

2844). Further experiments are needed, however, for a fuller understanding of the mechanism of retinal excitation by STS.

Long-Term Efficacy

The present study convinced us that it is feasible to develop an STS-based artificial retina for visually impaired people with degeneration of the outer retina, such as patients with RP and AMD. To reach this goal, however, the long-term stability and biocompatibility of implanted devices for STS have to be thoroughly examined. It is quite possible that regrowth or hypertrophy of the fenestrated sclera would cause deterioration of stimulating efficacy and resolution. Furthermore, prolonged stimulation of the choroid and the retina may induce pathologic changes, such as neovascularization or inflammation of the choriocapillaris. These changes may reduce the effectiveness of STS and even damage the retina. To evaluate the possible chronic effects of STS, we are currently developing surgical procedures for suprachoroidal implantation of a microelectrode array in cats and rabbits.

Acknowledgments

The authors thank Mitsuru Wada for major assistance with many experiments, Jun-Sub Choi for histologic analysis, and Tomomitsu Miyoshi, Tetsuya Yagi, and Masayuki Yamashita for valuable discussion and comments.

References

1. Tassicker GE. Retinal Stimulator. U.S. Patent 1956, No. 2, 760, 483.
2. Margalit E, Maia M, Weiland JD, et al. Retinal prosthesis for the blind. *Surv Ophthalmol.* 2002;47:335-356.
3. Zrenner E. Will retinal implants restore vision? *Science.* 2002;295: 1022-1025.
4. Rizzo JF, Wyatt J, Humayun M, et al. Retinal prosthesis: an encouraging first decade with major challenges ahead. *Ophthalmology.* 2001;108:13-14.
5. Lakhanpal RR, Yanai D, Weiland JD, et al. Advances in the development of visual prostheses. *Curr Opin Ophthalmol.* 2003;14: 122-127.
6. Chow AY, Chow VY. Subretinal electrical stimulation of the rabbit retina. *Neurosci Lett.* 1997;225:13-16.
7. Schwahn HN, Gekeler F, Kohler K, et al. Studies on the feasibility of a subretinal visual prosthesis: data from Yucatan micropig and rabbit. *Graefes Arch Clin Exp Ophthalmol.* 2001;239:961-967.
8. Hesse L, Schanze T, Wilms M, Eger M. Implantation of retina stimulation electrodes and recording of electrical stimulation responses in the visual cortex of the cat. *Graefes Arch Clin Exp Ophthalmol.* 2000;238:840-845.
9. Walter P, Heimann K. Evoked cortical potentials after electrical stimulation of the inner retina in rabbits. *Graefes Arch Clin Exp Ophthalmol.* 2000;238:315-318.
10. Schanze T, Wilms M, Eger M, Hesse L, Eckhorn R. Activation zones in cat visual cortex evoked by electrical retinal stimulation. *Graefes Arch Clin Exp Ophthalmol.* 2002;240:947-954.
11. Humayun MS, de Juan E Jr, Dagnelie G, Greenberg RJ, Propst RH, Phillips DH. Visual perception elicited by electrical stimulation of retina in blind humans. *Arch Ophthalmol.* 1996;114:40-46.
12. Humayun MS, de Juan E Jr. Artificial vision. *Eye.* 1998;12:605-607.
13. Weiland JD, Humayun MS, Dagnelie G, de Juan E Jr, Greenberg RJ, Iliff NT. Understanding the origin of visual percepts elicited by electrical stimulation of the human retina. *Graefes Arch Clin Exp Ophthalmol.* 1999;237:1007-1013.
14. Chow AY, Pardue MT, Perlman JI, et al. Subretinal implantation of semiconductor-based photodiodes: durability of novel implant designs. *J Rehabil Res Dev.* 2002;39:313-321.
15. Pardue MT, Stubbs EB Jr, Perlman JI, Narfstrom K, Chow AY, Peachey NS. Immunohistochemical studies of the retina following long-term implantation with subretinal microphotodiode arrays. *Exp Eye Res.* 2001;73:333-343.
16. Majji AB, Humayun MS, Weiland JD, Suzuki S, D'Anna SA, de Juan E Jr. Long-term histological and electrophysiological results of an inactive epiretinal electrode array implantation in dogs. *Invest Ophthalmol Vis Sci.* 1999;40:2073-2081.
17. Lederman RJ, Noell WK. Optic nerve population responses to transretinal electrical stimulation. *Vision Res.* 1969;9:1041-1052.
18. Potts AM, Inoue J. The electrically evoked response of the visual system (EER). 3: further contribution to the origin of the EER. *Invest Ophthalmol.* 1970;9:814-819.
19. Crapper DR, Noell WK. Retinal excitation and inhibition from direct electrical stimulation. *J Neurophysiol.* 1963;6:924-947.
20. Shimazu K, Miyake Y, Watanabe S. Retinal ganglion cell response properties in the transcorneal electrically evoked response of the visual system. *Vision Res.* 1999;39:2251-2260.
21. Siminoff R, Schwassmann HO, Kruger L. An electrophysiological study of the visual projection to the superior colliculus of the rat. *J Comp Neurol.* 1966;127:435-444.
22. Bourne MC, Campbell DA, Tansley K. Hereditary degeneration of the rat retina. *Br J Ophthalmol.* 1938;22:613-623.
23. LaVail MM. Legacy of the RCS rat: impact of a seminal study on retinal cell biology and retinal degenerative diseases. *Prog Brain Res.* 2001;131:617-627.
24. Bishop PO, McLeod JG. Nature of potentials associated with synaptic transmission in lateral geniculate of cat. *J Neurophysiol.* 1954;17:387-414.
25. Sefton AJ. The electrical activity of the anterior colliculus in the rat. *Vision Res.* 1969;9:207-222.
26. Usuda N, Kong Y, Hagiwara M, et al. Differential localization of protein kinase C isozymes in retinal neurons. *J Cell Biol.* 1991; 112:1241-1247.
27. Hughes A. A schematic eye for the rat. *Vision Res.* 1979;19:569-588.
28. Oyster CW. Ocular geometry and topography. In: *The Human Eye: Structure and Function.* Sunderland MA: Sinauer Associates, Inc., 1999:77-109.
29. Eisenfeld AJ, LaVail MM, LaVail JH. Assessment of possible transneuronal changes in the retina of rats with inherited retinal dystrophy: cell size, number, synapses, and axonal transport by retinal ganglion cells. *J Comp Neurol.* 1984;223:22-34.
30. Chu Y, Humphrey MF, Constable IJ. Horizontal cells of the normal and dystrophic rat retina: a wholemount study using immunolabelling for the 28-kDa calcium-binding protein. *Exp Eye Res.* 1993; 57:141-148.
31. Hartig W, Grosche J, Distler C, et al. Alterations of Muller (glial) cells in dystrophic retinae of RCS rats. *J Neurocytol.* 1995;24:507-517.
32. Hanitzsch R, Zeumer C, Lichtenberger T, et al. Impaired function of bipolar cells in the Royal College of Surgeons rat. *Acta Anat (Basel).* 1998;162:119-126.
33. Peng YW, Senda T, Hao Y, et al. Ectopic synaptogenesis during retinal degeneration in the Royal College of Surgeons rat. *Neuroscience.* 2003;119:813-820.
34. Villegas-Perez MP, Lawrence JM, Vidal-Sanz M, et al. Ganglion cell loss in RCS rat retina: a result of compression of axons by contracting intraretinal vessels linked to the pigment epithelium. *J Comp Neurol.* 1998;392:58-77.
35. Decker K, Disque-Kaiser U, Schreckenberger M, et al. Demonstration of retinal afferents in the RCS rat, with reference to the retinohypothalamic projection and suprachiasmatic nucleus. *Cell Tissue Res.* 1995;282:473-480.
36. Stett A, Barth W, Weiss S, Haemmerle H, Zrenner E. Electrical multisite stimulation of the isolated chicken retina. *Vision Res.* 2000;40:1785-1795.

Graefe's Arch Clin Exp Ophthalmol
(2005) 243: 169–174

LABORATORY INVESTIGATION

DOI 10.1007/s00417-004-1060-2

Kazuaki Nakauchi
Takashi Fujikado
Hiroyuki Kanda
Takeshi Morimoto
Jun S. Choi
Yasushi Ikuno
Hirokazu Sakaguchi
Motohiro Kamei
Masahito Ohji
Tohru Yagi
Shigeru Nishimura
Hajime Sawai
Yutaka Fukuda
Yasuo Tano

Transretinal electrical stimulation by an intrascleral multichannel electrode array in rabbit eyes

Received: 5 January 2004
Revised: 11 June 2004
Accepted: 19 September 2004
Published online: 7 December 2004
© Springer-Verlag 2004

H.K., T.Y., and S.N. are employees of NIDEK Co.

K. Nakauchi · T. Fujikado (✉) · H. Kanda · T. Morimoto
Department of Visual Science, Osaka University Graduate School of Medicine,
Room G4, 2-2 Yamadaoka, Suita-shi, Osaka, 565-0871, Japan
e-mail: fujikado@ophthal.med.osaka-u.ac.jp
Tel.: +81-6-68793941
Fax: +81-6-68793948

J. S. Choi · Y. Ikuno · H. Sakaguchi · M. Kamei · M. Ohji · Y. Tano
Department of Ophthalmology, Osaka University Graduate School of Medicine,
Suita,
Osaka, Japan

H. Sawai · Y. Fukuda
Department of Physiology, Osaka University Graduate School of Medicine,
Suita,
Osaka, Japan

H. Kanda · T. Yagi · S. Nishimura
NIDEK Co.,
Gamagori, Japan

Abstract *Background:* A new method of stimulating the retina electrically, called suprachoroidal transretinal stimulation (STS), was shown to be effective in eliciting electrically evoked cortical potentials (EEPs) in Royal College of Surgeons (RCS) rats. Before extending this technique to patients, it is important to determine its safety and feasibility in eliciting EEPs from medium-size animal (rabbits). The purpose of this study was to determine the safety and efficacy of the surgical procedures used to implant an multichannel electrode array into a scleral pocket, and to determine whether the implanted electrodes can stimulate the retina effectively. *Methods:* These acute experiments were conducted on six rabbits. An array of eight gold microelectrodes, embedded in polyimide, was implanted into a scleral pocket over the visual streak area. The size of the microarray was 2×4×0.180 mm. The reference electrode was implanted into the vitreous. The electrode array and reference electrodes were connected to a stimulator to deliver monophasic current pulses. Cortical responses were recorded with a stainless steel electrode implanted into each rabbit's skull over the visual cortex. After the experiment, the eyes and electrodes were examined histologically. *Results:* The surgical procedures for electrode implantation were accomplished without serious complications. EEPs were recorded after monophasic electrical pulse stimulation from each electrode. The mean threshold for EEPs was 55.0±10.0 μA with a 0.5-ms duration inward current pulse. The charge delivered at threshold was about 27.5 nC, and the charge density was about 56.0 μC/cm^2. Histopathological examination of the retinal tissue around the area of stimulation did not show damage at the light microscope level with the electrical parameters used. *Conclusions:* Our technique for STS with an intrascleral microelectrode array is safe in rabbit eyes, and EEPs were elicited by current densities that did not induce tissue damage. These results suggest that STS via intrascleral multichannel electrodes is a feasible method for stimulating the retina.

Introduction

Several research groups are currently developing electrode arrays that can be attached directly to the retina and used to stimulate the retina in an attempt to restore vision to patients with retinal degeneration [7, 11, 18]. In general, there are two types of retinal stimulating prosthesis: an epiretinal [5, 6, 10, 13, 16] and a subretinal [2, 3, 14, 17] prosthesis. Epiretinal stimulating prostheses are inserted into the vitreous cavity and attached to or placed against the inner retinal surface. The potential risk of this approach is the possible of a permanent attachment of the device to the retina. Epiretinal implantation can cause damage around the area of the retinal plug [10, 15] or may be unstable without the use of special methods to fix the electrodes [18]. Subretinal prostheses are placed between the pigment epithelial layer and the outer layer of the retina. The stability of this electrode is better but chronic implantation in this space might lead to a proliferation of glial tissue around the electrode array [17]. Although improvements in the surgical and electronic technologies may solve some of the problems of implanting retinal stimulating prostheses, the potential risk of significant damage to the eye after inserting an electrode intraocularly is significant.

To avoid the risks of damaging the retina by implanting a stimulating electrode array into the epi- or subretinal space, we have developed a new method of stimulating the retina called suprachoroidal transretinal stimulation (STS), with implantation of a stimulating electrode array in the suprachoroidal space. This method avoids direct contact of the electrodes with the retina. We have demonstrated that STS can elicit field responses at a defined areas of the superior colliculus which correspond retinotopically to the retinal region stimulated in both normal and blind Royal College of Surgeons (RCS) rats [9].

In the present study, we fabricated a multichannel electrode array and developed a surgical technique to insert the electrodes in a scleral pocket (intrascleral implanting method) in medium-sized animal (rabbits). The aims of this study were threefold: to determine the safety of this surgical technique, to establish the threshold current to elicit electrically evoked cortical potentials (EEPs), and to determine the retinal damage induced by the electrodes and by the electrical currents.

Materials and methods

Six pigmented rabbits (weighing 1.9–2.2 kg) were initially anesthetized with an intramuscular injection of ketamine hydrochloride (50 mg/kg) and xylazine hydrochloride (5 mg/kg). This amount of anesthetic kept the rabbits under a surgical level of anesthesia for 3 h. One eye was dilated with 0.5% tropicamide and 0.5% phenylephrine hydrochloride.

The procedures used on all animals conformed to the Institutional Guidelines of Osaka University and the ARVO Resolution on the Use of Animals in Research.

Stimulating electrodes

A photograph of the surface of the electrode array displaying the configuration of the electrodes is shown in Fig. 1. Eight dome-shaped microelectrodes (fabricated by NIDEK Co., Gamagori, Japan) were mounted in a polyimide strip, and the array was 2 mm wide, 4 mm long, and 180 μm thick. The dimensions of each electrode were as follows: height above the surface, 120–130 μm; diameter, 250 μm. The distance between electrodes was 500 μm. The impedance of the electrodes in saline is 10 kΩ at 1 kHz. The electrode array was connected to an external stimulator unit with insulated copper wires. Each electrode was coated with gold and was able to be activated separately.

Surgical method

The rabbit's eye was proptosed from the eye socket and draped with sterile rubberized cloth. After cutting the inferior half of the conjunctiva around the limbus, and cutting the inferior rectus and the inferior oblique muscles, the bare sclera was exposed. A scleral pocket (3×5 mm) was created just over the area of the visual streak, which was about 12 mm posterior to the limbus.

The multichannel electrode array was then implanted into the scleral pocket and sutured with 5-0 Dacron onto the sclera just above the pocket. The bundle of insulated leads from the microarray was also sutured at the limbus with 5-0 Dacron (Fig. 2). The surgical procedures took about 30 min.

An electronic stimulator (SEN-7203, Nihon Kohden, Shinjyuku, Japan) was then connected through an isolator (A-395R, World Precision Instruments, Sarasota, FL, USA) to the microelectrode array. The reference electrode was a platinum (Pt) wire coated with polyurethane resin and exposed at the tip. It was inserted 4 mm into the vitreous cavity and was fixed 2 mm from the limbus with 5-0 Dacron sutures.

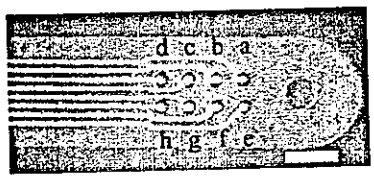

Fig. 1 Photograph of the electrode array. (*Scale bar* 1 mm). Eight gold electrodes (*a–h*) are mounted in a polyimide strip. Each electrode had the following dimension: height, 120–130 μm; diameter, 250 μm; impedance, 10 kΩ at 1 kHz. The distance between electrodes was 500 μm

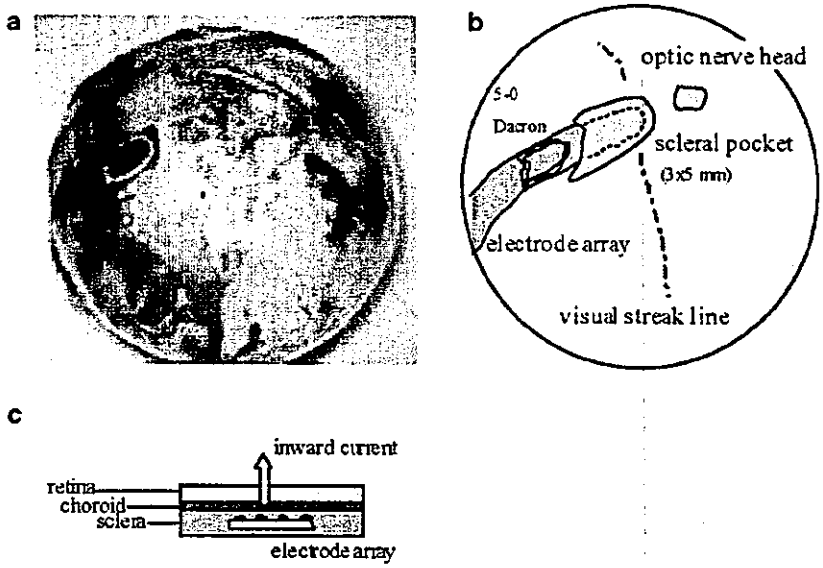

Fig. 2 a A photograph of an enucleated rabbit eye which has the microelectrode array implanted into the scleral pocket. b A schematic diagram of the electrode array that is inserted into a 3×5-mm scleral pocket over the visual streak. c A schematic diagram of transretinal electrical stimulation

Recording electrode

After exposing the skull, a stainless steel recording electrode was screwed into the skull bone above the visual cortex. The position of the electrode was 8 mm rostral to the lambda suture and 7 mm lateral to the midline [1, 8]. The reference needle stainless steel electrode was then placed between the skin and skull near the ear.

To confirm that the recording electrode was placed over the visual cortex, visual evoked potentials (VEPs) elicited by photic stimuli (1.2 J, 15 cm from the cornea) were recorded. The EEPs were elicited by monophasic electrical pulses of 0.5 ms duration, and 50 responses were averaged. A bandpass filter of 5 Hz to 1 kHz was used.

Electrical threshold current

The electric current was changed from 10 μA to 700 μA, and the direction of the current was first set for inward-flowing currents (electrode array positive and reference electrode negative), then the polarity was reversed for outward-flowing currents (electrode array negative and reference electrode positive).

For the purpose of finding the threshold current, the amplitudes of the EEPs elicited by a current of 500 μA delivered by each of the eight electrodes were compared. The electrode which elicited the largest EEP was selected to determine the threshold current. With this electrode, the electric current was decreased in steps, and the minimum electric current that elicited the first or second positive peak of the EEP (P_1 or P_2) was defined as the threshold current. The threshold current was also determined by reversing the polarity of the stimulating current.

Histology

At the completion of the experiment, the rabbit was killed by an overdose of barbiturate (100 mg/kg), and the eye was enucleated for histological examination. The eyes were embedded in paraffin, and 10-μm sections were cut and stained with hematoxylin and eosin (HE staining). Light microscopy was used to evaluate tissue damage. The electrode array used for stimulation was examined after the experiment with a scanning electron microscope.

Results

The electrode arrays were inserted and positioned without complications, and the placement of the recording electrode into the rabbit's skull was also completed without complications. Although the overall experiment time was only 3–4 h, early adverse effects were not detected in the eyes and brains surrounding the stimulating and recording electrodes.

The VEPs consisted of three large positive waves (Fig. 3a). The mean implicit time of the first positive peak (P_{v1}) was 23.8±1.2 ms, the second peak (P_{v2}) was 41.0± 3.0 ms, and the third peak (P_{v3}) was 58.2±2.1 ms (mean± SEM; n=6).

EEPs were also recorded in all rabbits. The mean implicit times of the EEP with an inward current (amplitude 500 μA; duration 0.5 ms) were 15.7±2.0 ms for P_{i1}, 27.3± 0.6 ms for P_{i2}, and 41.2±0.9 ms for P_{i3} (Fig. 3b). The implicit time of P_{i1} was significantly shorter than that for P_{v1}.

The waveform of EEPs with outward current with the same stimulus parameters consisted of four peaks, which were slightly different from that evoked by inward currents. The implicit times were 19.3±0.7 ms for P_{o1}, 30.1±

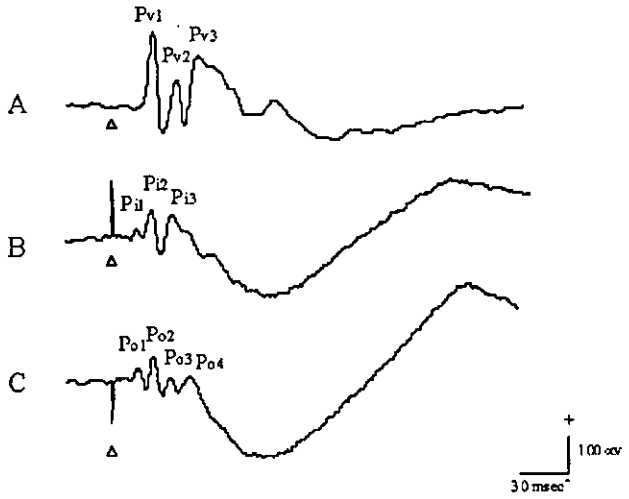

Fig. 3 Typical waveforms of VEP and EEPs. a VEP consists of three large positive components. The first positive peak (P_{v1}) had an implicit time of 24 ms, the second positive peak (P_{v2}) had an implicit time of 41 ms, and the third positive peak (P_{v3}) had an implicit time of 58 ms. b EEP with inward current (sclera+/vitreous−) shows an upward artifact at the onset of the stimulation. The first positive peak (P_{i1}) had an implicit time of 16 ms, a second positive peak (P_{i2}) had an implicit time of 27 ms, and a third positive peak (P_{i3}) had an implicit time of 41 ms. c EEP with outward current (sclera−/vitreous +) shows a negative downward artifact at the time of stimulation. The first positive peak (P_{o1}) had an implicit time of 19 ms, the second positive peak (P_{o2}) had an implicit time of 30 ms, a third positive peak (P_{o3}) had an implicit time of 42 ms, and a fourth positive peak (P_{o4}) had an implicit time of 59 ms

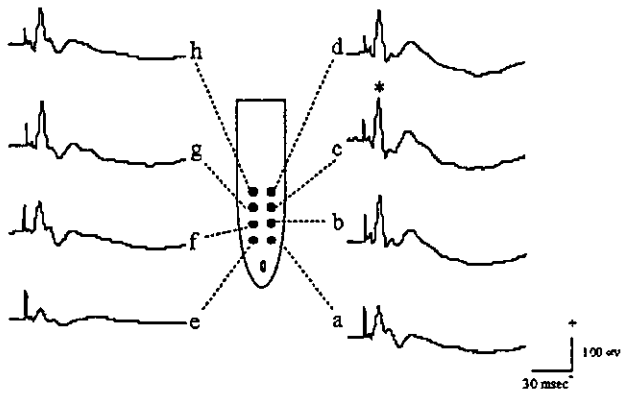

Fig. 4 EEPs elicited by inward electrical pulses from each of the eight electrodes. The amplitude of second positive peak (P_2) varies with the different electrodes. Because electrode *c* elicited the largest amplitude (*), electrode *c* was used for determining the threshold electrical current

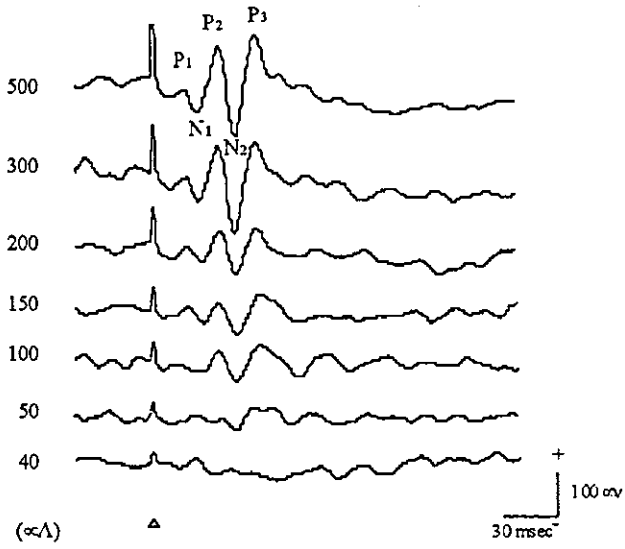

Fig. 5 Changes of the EEP waveforms with decreasing inward electrical currents for stimulation. The second and third positive peaks (P_2, P_3) were detectable with stimulus intensity ≤50 μA. The negative peaks (N_1, N_2) were detectable with stimulus intensity ≤100 μA

0.8 ms for P_{o2}, 41.6±0.9 ms for P_{o3}, and 59.0±0.7 ms for P_{o4} (Fig. 3c). The implicit times of P_{o1} and P_{o2} were slightly longer than P_{i1} and P_{i2}, but that of P_{o3} was not significantly different from that of P_{i3}.

The mean amplitude of the EEPs elicited by 500 μA inward current was 190±26 μV, while that for 500 μA outward current was 150±22 μV (n=6). Because the inward current elicited significantly larger EEPs, we selected the inward current for determining the thresholds.

The EEPs elicited by stimulating with each of the eight electrodes are compared in Fig. 4. Although the overall shape was similar for each of the electrodes, the peak amplitude of the second positive component (P_2) was different. The largest amplitude was elicited by stimulating with electrode c, and it was used for determining the threshold currents.

The EEPs elicited with decreasing inward currents are shown in Fig. 5. For the second (P_2) and third (P_3) peaks, the minimum stimulation current to elicit these peaks was obtained with 50 μA. For the negative components, the first negative peak (N_1) and the second negative peak (N_2) were obtained until 100 μA. The mean threshold current that elicited a small EEP was 55.0±10.0 μA for the six rabbits (27.5±5.0 nC).

The relationship between the averaged peak-to-peak amplitude (P_2 to N_2) of the EEPs and the inward current was examined in the six rabbits (Fig. 6). The regression curve showed that the EEP amplitude increased almost linearly with the lower stimulus currents and tended to be saturated with higher stimulus currents.

Histology

Examination of the histological sections surrounding the implanted electrode showed no obvious damage to the retina, choroid, and sclera at the light-microscopic level. Although a fissure was observed in the sclera which cor-

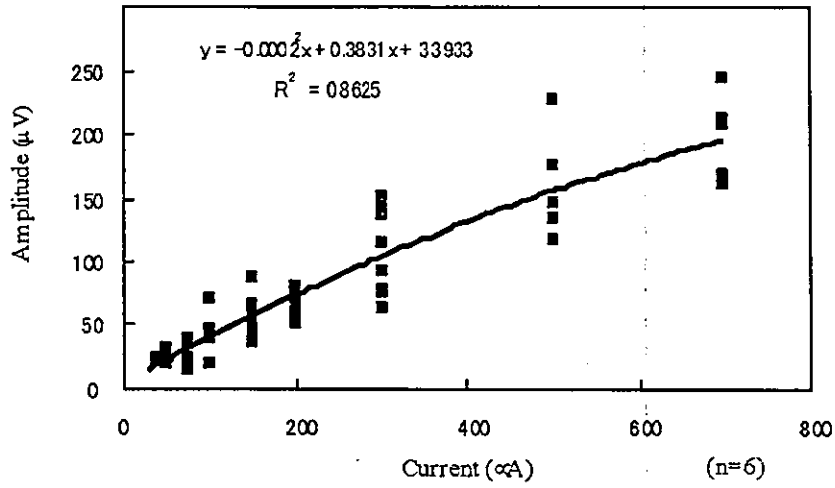

Fig. 6 Averaged peak-to-peak (from P_2 to N_2) amplitude (ordinate) of retinal response elicited by increasing inward current stimulation (*abscissa*). The regression curve shows a slow increase of EEP amplitude with stimulus current amplitude. The increase in the response amplitude is approximately linear with low stimulus current and tended to be saturated with greater stimulus currents

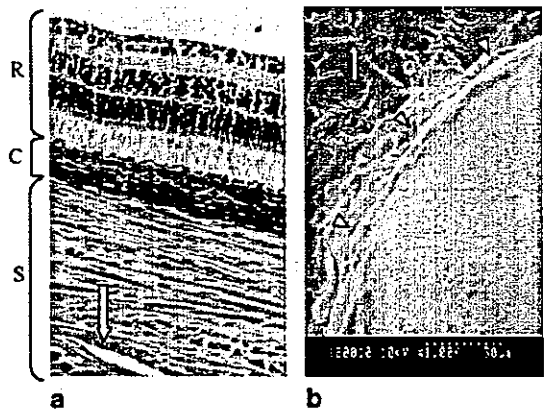

Fig. 7 **a** Histology of the retina and sclera around the electrode. The retina shows no significant damage around the area attached to the array. Degeneration and vacuolization cannot be seen in the sclera and retina. The *arrow* shows the edge of the scleral pocket. *R* Retina, *C* choroids, *S* sclera. HE staining, ×200. **b** A photograph of electrode array surface by scanning electron microscopy. The *arrowheads* point to the electrode surface. There is no deterioration such as cracks on the electrode, only dried crystals (*arrow*) of tissue fluids beside the electrode

responded with the scleral pocket, no significant tissue damage was observed in the sclera (Fig. 7a).

Scanning electron microscopic examination of the electrode also showed no evidence of electrode deterioration such as cracks on the electrode surface but only dried crystals of tissue fluids beside the electrode (Fig. 7b).

Discussion

In this study, we implanted a multichannel electrode array into the sclera. The implantation of electrodes intrasclerally was not difficult, and neither retinal hemorrhage nor retinal detachment was observed during or after the surgery, which suggests the safety of the surgical procedures.

The rabbit retina could be stimulated by STS using electrical currents from multichannel electrodes. The threshold charge for eliciting EEP was 27.5 nC, which is equivalent to a charge density of 56.0 $\mu C/cm^2$. Humayun et al. reported that a charge density of 8.92–11.9 $\mu C/cm^2$ was required to elicit EEPs from rabbits with epiretinal electrodes [6]. In experiments on cats, Dawson and Radtke found a threshold charge density of 30.5 $\mu C/cm^2$ [4]. Chow and Chow implanted their electrodes subretinally in rabbits and reported a threshold charge density of 2.8 nC/cm^2 to elicit EEPs [2]. Although the distance from the electrodes to the retina was farther for our transscleral electrodes than for epi- or subretinal electrodes, the threshold charge density to elicit EEPs was comparable with the other electrode placements.

After changing the polarity to outward currents, the mean threshold was elevated to 75.0 μA (37.5 nC), which was higher than that for inward currents. This finding is consistent with our previous reports that the threshold of inward currents was lower than that of outward currents to elicit EEPs in rats [9].

McCreery et al. reported that the electric charge which can elicit EEPs without damaging the neural tissue was 50 nC or an electrical charge density of 10 $\mu C/cm^2$ [12]. This is thought to be the borderline for chronic clinical stimulation; thus, it was recommended that the stimulating electrical current be kept below this charge density. For our system, the electrical charge current was at the upper limit of this borderline, but the charge density exceeded the borderline. Our stimulation method was not a direct stimulation of neural tissue, but an indirect transretinal stimulation. Therefore, the limit of electrical charge density may be expected to be higher than that with direct retinal stimulation.

The retinal origin of EEPs evoked by STS is still unknown. Our previous report [9] showed that STS elicited EEPs without photoreceptors in RCS rat, suggesting that

STS can stimulate the inner retinal neurons. In this study, paying attention to the implicit time of the first EEP peak (P_1) was shorter than that of the first VEP peak (P_{v1}), which suggested that the neuronal processes underlying EEPs by our method were faster than those involved in light stimulation. This shorter implicit time suggests again that STS had elicited EEP by stimulating the inner layers of normal rabbit retina.

The EEP waveforms elicited by intrascleral stimulation were similar to the EEPs elicited by subretinal stimulation [2, 14] or by epiretinal stimulation [13, 16]. They all had several fast wavelets followed by a large slow wave with a latency around 100 ms. Thus, we conclude that we can stimulate the same neural components by intrascleral transretinal stimulation as by epi- or subretinal stimulation.

Our histopathological examinations showed that no obvious damage occurred at the light-microscopic level in the retinal and scleral tissues with the electrical currents used in these acute experiments. Scanning electron microscopy showed no deterioration such as cracks on the used electrode surface. These results showed that the threshold of electric current was low enough to preserve the retinal tissue, and that our stimulating method was also safe.

Although some researchers have reported that the epiretinal [15] and subretinal [3] methods are safe for the retinal tissue, subretinal implantation can cause damage to the outer segments of photoreceptors [14] and induce glial proliferation when chronically implanted [17]. Epiretinal implantation can cause damage around the area of the retinal plug [10, 15], or may be unstable without the use of special devices to fix the electrodes [18]. Our method, on the other hand, requires only scleral surgery and there is no direct invasion of retinal tissue. This simplicity makes the intrascleral electrode insertion a safe and promising method.

In conclusion, our novel surgical procedure, an intrascleral implantation method for STS, represents a safe method for implanting an electrode array in rabbit eyes. EEPs were elicited from the visual cortex with a low electrical current, and the tissue damage was minimal around the electrode. In the future, this method has a potential of increasing the number of electrodes. However, additional studies are necessary to determine the spatial resolution and the long-term effects on the surrounding tissues.

Acknowledgements This study was supported by Health Science Grant, Japan, and by a grant (No. 14571670) from the Ministry of Education, Culture, Sports, Science and Technology, Japan.

References

1. Choudhury DP (1978) Visual field representation in the newborn rabbit's cortex. Brain Res 153:27–37
2. Chow AY, Chow VY (1997) Subretinal electrical stimulation of the rabbit retina. Neurosci Lett 225:13–16
3. Chow AY, Pardue MT, Perlman JI, Ball SL, Chow VY, Helting JR, Peyman GA, Liang C, Stubbs EB Jr, Peachey NS (2002) Subretinal implantation of semiconductor-based photodiodes: durability of novel implant designs. J Rehabil Res Dev 39:313–322
4. Dawson WW, Radtke ND (1977) The electrical stimulation of the retina by indwelling electrodes. Invest Ophthalmol Vis Sci 16:249–252
5. Eckmiller R (1997) Learning retina implants with epiretinal contacts. Ophthalmic Res 29:281–289
6. Humayun MS, Probst R, de Juan E Jr, McCormick K, Hickingbotham D (1994) Bipolar surface electrical stimulation of the vertebrate retina. Arch Ophthalmol 114:40–46
7. Humayun MS (2001) Intraocular retinal prosthesis. Trans Am Ophthalmol Soc 99:271–300
8. Inoue J, Potts AM (1971) Electrically evoked response of the visual system (EER) in the rabbit. Nippon Ganka Gakkai Zasshi 20(75):765–772
9. Kanda H, Morimoto T, Fujikado T, Tano Y, Fukuda Y, Sawai H (2004) Electrophysiological studies on the feasibility of suprachoroidal–transretinal stimulation for artificial vision in normal and RCS rats. Invest Ophthalmol Vis Sci 45:560–566
10. Majji AB, Humayun MS, Weiland JD, Suzuki S, D'anna SA, de Juan E Jr (1999) Long-term histological and electrophysiological results of an inactive epiretinal electrode array implantation in dogs. Invest Ophthalmol Vis Sci 40:2073–2081
11. Margalit E, Maia M, Weiland JD, Greenberg RJ, Fujii GY, Torres G, Piyathaisere DV, O'Hearn TM, Liu W, Lazzi G, Dagnelie G, Scribner DA, de Juan E Jr, Humayun MS (2002) Retinal prosthesis for the blind. Surv Ophthalmol 47:335–356
12. McCreery DB, Agnew WF, Yuen TG, Bullara L (1990) Charge density and charge per phase as cofactors in neural injury induced by electrical stimulation. IEEE Trans Biomed Eng 37:996–1001
13. Nadig MN (1999) Development of a silicon retinal implant: cortical evoked potentials following focal stimulation of the rabbit retina with light and electricity. Clin Neurophysiol 110:1545–1553
14. Schwahn HN, Gekeler F, Kohler K, Kobuch K, Sachs HG, Schulmeyer F, Jakob W, Gabel VP, Zrenner E (2001) Studies on the feasibility of a subretinal visual prosthesis: data from Yucatan micropig and rabbit. Graefes Arch Clin Exp Ophthalmol 239:961–967
15. Walter P, Szurman P, Viobig M, Berk H, Ludtke-Handjery H-C, Deng HR, Mittermayer C, Heimann K, Sellhaus B (1999) Successful long term implantation of electrically inactive epiretinal microelectrode arrays in rabbits. Retina 19:546–552
16. Walter P, Heimann K (2000) Evoked cortical potential after electrical stimulation of the inner retina in rabbits. Graefes Arch Clin Exp Ophthalmol 238:315–318
17. Zrenner E, Stett A, Weiss S, Aramant RB, Guenther E, Kohler K, Miliczek KD, Seiler MJ, Haemmerle H (1999) Can subretinal microphotodiodes successfully replace degenerated photoreceptors? Vision Res 39:2555–2567
18. Zrenner E (2002) Will retinal implants restore vision? Science 295:1022–1025

Available online at www.sciencedirect.com
SCIENCE DIRECT®
Vision Research 45 (2005) 263–273
Vision Research
www.elsevier.com/locate/visres

Temporal properties of retinal ganglion cell responses to local transretinal current stimuli in the frog retina

Liming Li [1], Yuki Hayashida [2], Tetsuya Yagi *

Graduate School of Life Science and Systems Engineering, Kyushu Institute of Technology, Hibikino 1-1, Wakamatsu, Kitakyushu 808-0196, Japan

Received 23 January 2003; received in revised form 16 March 2004

Abstract

Extracellular current stimuli have been used in both electrophysiological and clinical studies. The present study elucidates the temporal properties of the frog retinal ganglion cell response induced by local transretinal current stimuli. Two classes of spike response were recorded from the ganglion cell. One had a constant latency ranging from 1.5 to 4.5 ms after the onset of the stimulus regardless of differences in stimulus parameters. Another class had a latency that varied from trial to trial between 3.5 and 71.5 ms at the threshold even when stimulus parameters were identical. The latency became shorter and the number of spike responses increased as the charge applied via the stimulus pulse was increased by increasing the amplitude (from 50 to 200 μA) or the pulse duration (from 100 to 1000 μs). In both classes, the current stimuli with the same amount of charge induced responses of a similar latency for amplitudes between 50 and 200 μA and for pulse durations between 100 and 1000 μs.
© 2004 Elsevier Ltd. All rights reserved.

Keywords: Retina; Ganglion cells; Prosthesis; Current stimulus; *Multielectrode*

1. Introduction

Extracellularly applied electrical stimuli have been used to study neuronal mechanisms of various nerve tissues including the retina. Recently, the externally applied electrical stimulus has been considered as a means to excite retinal neurons of blind patients suffering from degenerative retinal diseases, such as retinitis pigmentosa and age related macular degeneration (Chow & Chow, 1997; Eckmiller, 1997; Humayun, Sato, Propst, & de Juan, 1995; Humayun et al., 1996; Peyman et al., 1998; Rizzo & Wyatt, 1997; Wyatt & Rizzo, 1996; Zrenner, 2002; Zrenner et al., 1997; Zrenner et al., 1999). Accordingly, the effects of amplitude, duration and waveform of current or voltage pulses applied diffusely to the retina were examined in ganglion cells (Grumet, Wyatt, & Rizzo, 2000; Humayun, 2001; Stett, Barth, Weiss, Haemmerle, & Zrenner, 2000), in visual cortex neurons (Hesse, Schanze, Wilms, & Eger, 2000) as well as in visual perception (Humayun et al., 1996; Humayun et al., 1999; Weiland et al., 1999). The effects of external current stimuli applied with two electrodes placed either at the inner retinal surface or at the photoreceptor side were also examined (Chow & Chow, 1997; Humayun, Propst, de Juan, McCormick, & Hickingbotham, 1994; Humayun, 2001; Humayun et al., 1996; Humayun et al., 1999; Walter & Heimann, 2000).

A transretinal current applied diffusely over the retinal tissue is known to cause several types of retinal neurons

* Corresponding author. Present address: Tetsuya Yagi, Graduate School of Engineering, Osaka University, Yamada-Oka 2-1, Suita, Osaka 565-0871, Japan. Tel.: +81-6-6879-7785.
E-mail address: yagi@ele.eng.osaka-u.ac.jp (T. Yagi).
[1] Present address: Department of Psychology, Graduate School of Humanities and Sociology, The University of Tokyo, 7-3-1 Hongo, Bunkyo-ku, Tokyo 113-0033, Japan.
[2] Present address: Section of Neurobiology, Physiology, and Behavior, University of California, One Shields Avenue, Davis, CA 95616, USA.

0042-6989/$ - see front matter © 2004 Elsevier Ltd. All rights reserved.
doi:10.1016/j.visres.2004.08.002

to release neurotransmitters and give rise to voltage responses in postsynaptic neurons. Voltage responses were observed in the second order neurons, i.e., horizontal cells and bipolar cells, when the retina was stimulated with a current flowing from the receptor side to the vitreous side (Kaneko & Saito, 1983; Toyoda & Fujimoto, 1984; Toyoda, Fujimoto, & Saito, 1977; Trifonov, 1968). It has been also demonstrated that the calcium conductance was activated in horizontal cells (Byzov & Trifonov, 1968; Murakami & Takahashi, 1987) and amacrine cells (Takahashi & Murakami, 1988) when transretinal current was applied over entire retina. The effect of transretinal current, however, is not well characterized when applied locally to the retinal circuit.

In both the physiological and the clinical aspects, it is important to clarify the effect of locally applied external electrical stimuli since the extracellular stimuli given by electrodes with different arrangements might excite neurons by different mechanisms, and therefore elicit responses of different properties (Greenberg, Velte, Humayun, Scarlatis, & de Juan, 1999; Ranck, 1975). In the present paper, we elucidated temporal properties of ganglion cell responses to local current stimuli applied using two electrodes placed transretinally in the frog retina. Preliminary results have been presented in abstract form (Li, Kameda, Hayashida, & Yagi, 2001).

2. Methods

2.1. Retina preparation

Bullfrogs (*Rana Catesbeiana*, 9.5–11 cm in length) were dark adapted for 1–1.5 h and pithed under dim illumination. Eyeballs were enucleated and hemisected. After the cornea and lens were removed, sclera was separated from the pigment epithelium. The retina was then isolated from the pigment epithelium. A piece of the retina about 2–3 mm width was cut from the central part of the retina. The piece of the retina was then positioned with photoreceptor side up on the surface of a planar electrode array. The planar electrode array was fabricated at the center of a glass chamber as illustrated in Fig. 1A (MED probe, Matsushita Electronic Industrial Co., LTD, Japan) (Oka, Shimono, Ogawa, Sugihara, & Taketani, 1999). After rinsing the retina with the Ringer solution, the Ringer was removed from the chamber and the retina was fixed by a plastic ring-shaped frame covered with a tightly stretched piece of mesh. The composition of Ringer solution was (in mM): NaCl 100, KCl 3.3, $CaCl_2$ 2, $MgCl_2$ 1, Glucose 10, HEPES 10. During the experiment, the recording chamber, covered with a transparent plastic dish, was continuously supplied with a moist gas (98% O_2 and 2% CO_2).

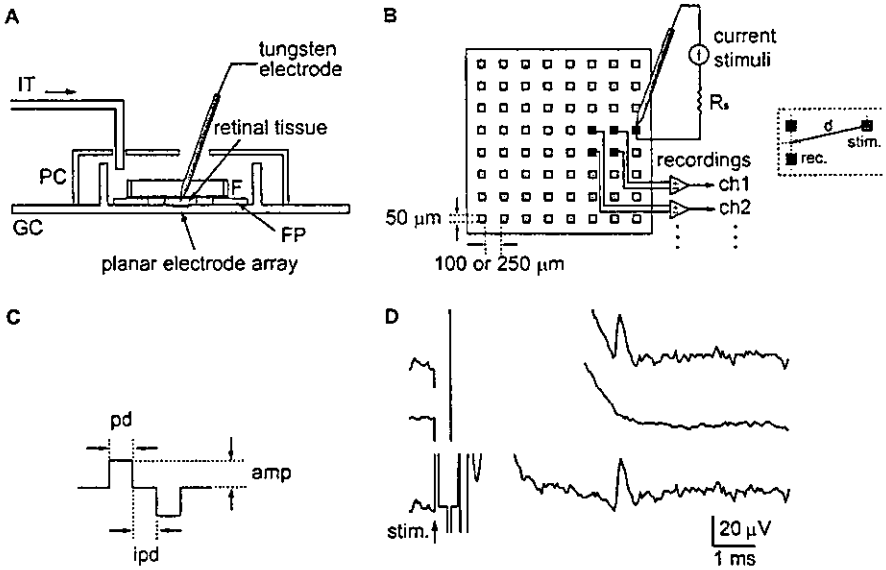

Fig. 1. Diagram of recording and stimulation system. (A) Side view of the system. A moist gas, 98% O2 and 2% CO2, was supplied via the inlet tube (IT) inside the chamber with a plastic cover (PC). GC, glass chamber; F, ring-shaped frame covered with a piece of mesh; FP, ring-shaped filter paper. (B) Top view of the system. Responses of ganglion cells were recorded by six pairs of neighboring electrodes simultaneously. Two types of electrode array with different spacing, 100 and 250 μm, were used in this study. Inset: Distance between the stimulus and the recording sites, d, was defined as the distance between the center of the planar electrode for stimulation and that of the pair of recording electrodes. (C) Current stimulus. A charge-balanced biphasic square current stimulus was used to stimulate the retina. Amp, pd and ipd represents the current amplitude, the pulse duration, and the inter-pulse duration, respectively. The waveform of the current stimulus was monitored during the experiment by measuring the voltage across a 10 kΩ resistor, seen in (B) as Rs, inserted in series with the tungsten electrode.(D) Reduction of artifacts. The middle trace, a template trace, was subtracted from the top trace. The template is an averaged response of recordings obtained from the same electrode pair with subthreshold stimuli. The difference between the top and the middle traces is shown in the bottom trace.

2.2. Planar electrode array

The planar electrode array consists of 64 electrodes arranged in an 8 × 8 array (Fig. 1B). Each electrode is made of gold (50 nm in thickness), the surface of which is covered with platinum black to reduce impedance (Oka et al., 1999). The size of each electrode is 50 × 50 μm. The impedance of the electrode at first use is 50 kΩ or less for a 1 kHz, 50 mV sinusoidal wave. The impedance of the electrode generally increases after repeated use.

2.3. Stimulus

To examine the capability of recording ganglion cell responses in each planar electrode, the retina was illuminated with a full-field diffuse light of a green LED (TLGD240P, Toshiba Company, Japan, peak wavelength 567 nm) before the current stimulus was applied to the retina. A square wave with a frequency of 0.2 Hz was used to induce the ganglion cell responses (Ishikane, Kawana, & Tachibana, 1999). The light-induced responses were checked on each electrode. The electrodes, in which light-induced responses were observed, were picked up to record the electrically induced responses. This procedure, however, does not exclude the possibility of recording the electrically induced responses from ganglion cells that do not respond to the diffuse light.

After recording the light-induced responses of ganglion cells, local current stimuli were applied transretinally between a tungsten electrode inserted into the outer retina and one of the planar electrodes underneath the tungsten electrode (bipolar stimulation mode) as shown in Fig. 1A and B. The position of the tungsten electrode tip was controlled by a micromanipulator (MM-220, NARISHIGE) and monitored under a microscope. The tungsten electrode was placed on the surface of the retina. In some cases, the tungsten electrode was inserted up to 100 μm from the surface but no significant difference was observed in the recorded ganglion cell response. The tungsten electrode had an impedance of 0.5 MΩ and the length of the electrically exposed tip was about 50 μm (TM33B05, World Precision Instruments).

The current stimulus was a charge-balanced biphasic square pulse as shown in Fig. 1C. The charge-balanced stimulus is thought to be less noxious to neural tissue than the monophasic stimulus (Bartlett, Doty, Lee, Negrao, & Overman, 1977; Brummer & Turner, 1977; Lilly, Hughes, Alvord, & Galkin, 1955; Margalit et al., 2002; Tehovnik, 1996). The current stimulus was generated by a computer-controlled isolator (Model BSI-2, Bak Electronics Inc., Japan). The amplitude (amp), pulse duration (pd) and inter-pulse duration (ipd) of current stimulus were varied to examine the effects of these parameters on the electrically induced responses. The waveform of the current stimulus was monitored during the experiment by measuring the voltage across a 10 kΩ resistor inserted in series to the tungsten electrode (Fig. 1B). The stimuli of equivalent parameters were repetitively applied 10 times every 2 s.

2.4. Recording

To reduce the artifact and noise, a pair of neighboring electrodes was used to record the responses of retinal ganglion cells (differential recording configuration, Fig. 1B). Voltage recordings with a monopolar electrode (reference electrode in the bath) usually produce large artifacts due to the electrical stimuli that mask ganglion cell responses induced within 10 ms after stimulus onset. The artifact can be prominently reduced by taking the difference of monopolar recordings using a differential recording configuration (Data not shown). Responses were recorded simultaneously using six pairs of electrodes. The signals recorded by the electrodes were fed to 8-channel head- and main- amplifiers after being bandpass-filtered (0.1–5 kHz). The signals were then sampled at a rate of 20 kHz per channel and stored in the computer.

In some data analyses, the signal obtained by differential recording, in which the spike activities were absent, was subtracted from those with spike activities to further reduce artifacts as shown in Fig. 1D. The upper trace shows a spike recorded by a pair of electrodes. The middle trace is an averaged recording obtained with subthreshold stimuli from the same electrode pair. The lower trace is obtained by subtracting the middle trace from the upper trace.

Spontaneous spike discharges were seldom observed in the frog retina. When spontaneous discharges were observed, the electrically induced responses were discriminated by excluding the responses that showed similar waveforms to those of the spontaneous responses.

3. Results

3.1. Light-induced responses

Fig. 2 shows ganglion cell responses of dark-adapted retinas to a full-field diffuse illumination recorded by a pair of electrodes. Spike discharges were observed at either light on and/or off. In most cases (76 out of 94 recordings from 17 retinas), a higher frequency of spike discharges was observed when the light was turned off compared with on (Fig. 2A). Only off responses were observed in the rest of the recordings (Fig. 2B).

Waveforms of spikes are shown in Fig. 2C and D. These waveforms were obtained from the spikes whose amplitudes were more than three times larger than the standard deviation of the baseline fluctuations of each

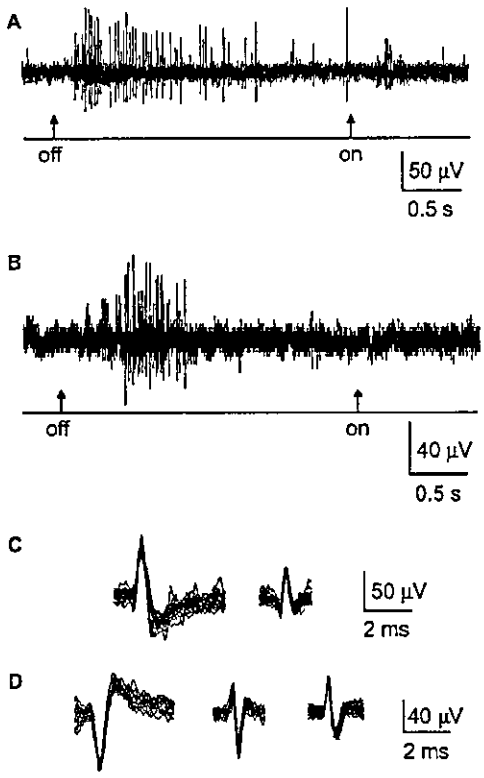

Fig. 2. Light induced responses of ganglion cells to a full-field diffuse illumination. Off and on in A and B stands for the time when the light was turned off and on, respectively. (A) On and off response. The light intensity was 6.8×10^{10} photons$s^{-1}cm^{-2}$. (B) Off response. The light intensity was 1.2×10^{10} photons$s^{-1}cm^{-2}$. (C) Biphasic and triphasic spikes recorded in this study. (D) Spike waveforms with opposite phases than those in (C). A narrow biphasic spike (right) was recorded as well. Spikes recorded in one illumination cycle (5 s) were superimposed in (C) and (D).

trial. As shown in Fig. 2C, some spikes showed a biphasic waveform with an initial positive phase lasting 0.5–1.0 ms followed by a longer duration negative phase (left). Another type showed a triphasic waveform (right) in which the width of the central phase was 0.2–0.4 ms and the whole width of the spike was 1.0–2.0 ms. Biphasic and triphasic spikes with reversed polarity (Fig. 2D, left and middle), as well as narrow biphasic spikes (Fig. 2D, right), were also recorded in this study.

3.2. Electrically induced responses

Ganglion cell responses to local transretinal current stimuli with different parameters were examined. In most cells (56 out of 58 cells in 13 retinas), the response showed all-or-none properties. In only 2 out of 58 cells in two retinas, the amplitude of the electrically induced response varied when current stimulus parameters were altered (Data not shown). Two fundamentally different classes of all-or-none responses were observed. One class showed a parameter invariant constant latency. The second class showed variable latencies.

3.2.1. Responses with constant latency

Fig. 3 shows an example of a constant latency response. Similar recordings were observed from five cells in three retinas. In Fig. 3A, the response to a stimulus with varying amplitude (10–100 μA) is shown. The stimulus was repeated 10 times at each set of parameters. The recordings of 10 trials are superimposed in each trace. As shown in the figure, no obvious response was observed when the amplitude of current stimulus was 10 μA (upper trace). A spike response was observed in each trial when the current amplitude was increased to 50 μA (middle trace). The waveform of the spike was triphasic. The latency of the spike response was 4.38 ± 0.04 ms (mean ± SD, the same below, 10 trials) in this case. The latency of the spike changed little (4.26 ± 0.03 ms, 10 trials) by a further increase in current amplitude to 100 μA (lower trace). A single spike was observed in each trial.

The effects of the stimulus pulse duration on this class of response were examined on the same ganglion cell (Fig. 3B). The pulse duration of current stimulus was varied from 100 to 500 μs. As shown in the figure, no obvious spike was observed when the pulse duration was 100 μs (upper trace). Upon increasing the pulse duration to 200 μs, a spike was elicited in every trial (middle trace). The latency was 4.45 ± 0.03 ms (10 trials) in this case, varying little (4.51 ± 0.02 ms, 10 trials) when the pulse duration was further increased to 500 μs (lower trace).

Fig. 3C shows the effects of the inter-pulse duration on the response of the same ganglion cell. The inter-pulse duration of current stimulus was varied from 0 to 1000 μs. No obvious spike was observed when there was no inter-pulse duration in the stimulus (upper trace). When the inter-pulse duration was increased to 500 (middle trace) or to 1000 μs (lower trace), the spike with a latency of 4.37 ± 0.03 ms (10 trials) or 4.39 ± 0.04 ms (10 trials) was elicited in each trial. The latency of the spike was not affected by the inter-pulse duration, suggesting that the spike was triggered by the first positive pulse. These results indicated that stimuli with shorter inter-pulse durations were less effective in exciting the ganglion cell.

3.2.2. Responses with variable latency

Another class of response had a variable latency. The latency of the response varied among 10 trials of identical stimulus parameters. The latency became shorter as the amplitude of the stimulus increased in this class (26 cells in 10 retinas). Fig. 4 illustrates the effects of the stimulus amplitude. The amplitude of stimulus was increased from 10 to 200 μA in this experiment. Each trace in A illustrates the superimposed responses of 10

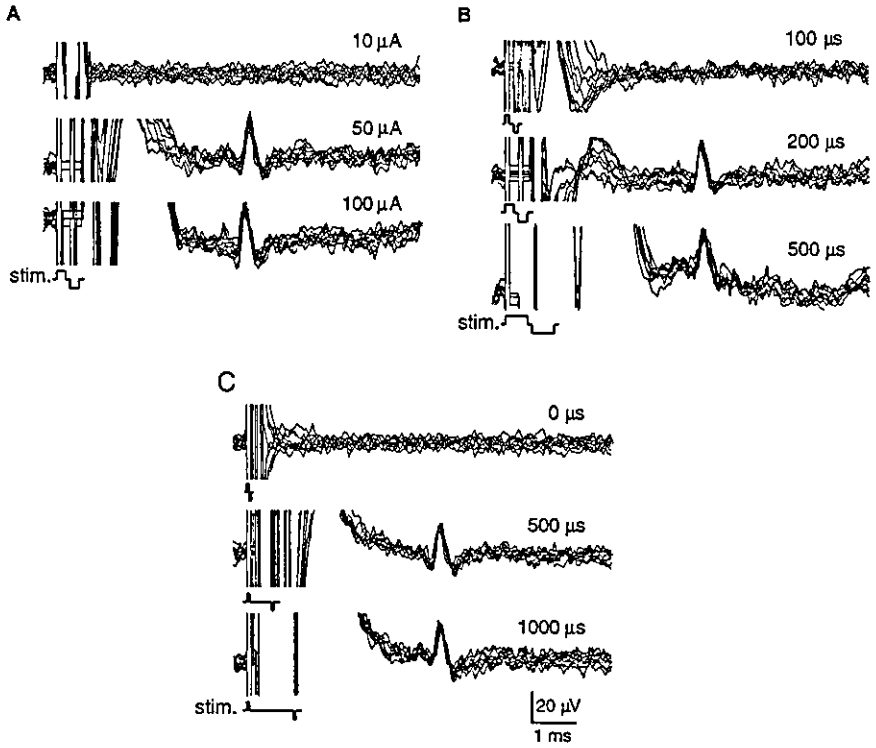

Fig. 3. Electrically elicited responses with a constant latency. All the responses were recorded from the same ganglion cell. The distance between the center of the planar stimulation electrode and that of the pair of recording electrodes (see Fig. 1B) is 270μm. Each trace is the superposition of recordings of 10 trials. (A) Effect of stimulus amplitude on cell response. The pulse and the inter-pulse durations of stimuli were fixed at 200 and 100 μs, respectively. (B) Effect of stimulus pulse duration on cell response. The amplitude and the inter-pulse duration of stimuli were fixed at 50 μA and 100 μs, respectively. (C) Effect of stimulus inter-pulse duration on cell response. The amplitude and the pulse duration of stimuli were fixed at 100 μA and 50 μs, respectively. The total amount of charge applied per phase of the stimulus was 5 nC.

trials. As shown in the figure, no obvious spike was observed when the stimulus amplitude was 10 μA (first row). Spike responses with latency of 51.7 ms and of 60.8 ms were observed in the first and fifth trials at the amplitude of 50 μA (second row). When the amplitude of the stimulus was increased to 100 μA (third row), a single spike was elicited in every trial and the latency became shorter (26.2 ± 4.8 ms, 10 trials). As the stimulus amplitude was increase to 200 μA, the second spike appeared in each trial (fourth row). The latency of the first spike was 13.8 ± 0.8 ms (10 trials) and that of the second one was 25.1 ± 2.1 ms (10 trials) in this case. It is notable that the locally applied single biphasic transretinal current pulse can give rise to a single spike when its parameters are appropriately adjusted.

The waveforms of the spike responses recorded in Fig. 4A are shown in an expanded time scale in Fig. 4B. In the upper trace (a), the waveforms of the two spikes induced by the 50 μA stimulus are superimposed. The middle trace (b) shows ten spikes induced by the stimulus of 100 μA superimposed. The lower traces (c) and (d) show spikes induced by the stimulus of 200 μA superimposed. The first spike is shown in (c) and the second in (d). The similarity of the waveforms shown in B indicated all the spikes were recorded from the same ganglion cell. In this recording, the waveform of the spike was biphasic. A majority of cells (30 out of 51) showed a clear biphasic waveform. A triphasic waveform was also observed in 4 cells in this response class. The remaining cases were not discernible because of the fluctuation of the base line. When the amplitude of stimulus was increased to 200 μA, the fluctuation of the base line due to small spike activities increased, suggesting that the number of cells excited by the stimulus increased. Raster plots of 10 trials at each current amplitude (Fig. 4C) show that the latency becomes shorter and the deviation of the latency becomes smaller as the amplitude of the stimulus increases.

Fig. 5 shows effects of the pulse duration on responses with a variable latency. As shown in the figure, similar effects as Fig. 4 were observed (16 cells in 6 retinas) when the pulse duration of the stimulus was increased from 100 to 1000 μs. Each trace in A is the superimposed response of 10 trials. B shows raster plots of the spikes. No obvious spike was elicited when the pulse duration was 100 μs. A single spike was induced in 9 trials, when the pulse duration was increased to 500 μs. In one trial (sixth trial), the second spike with

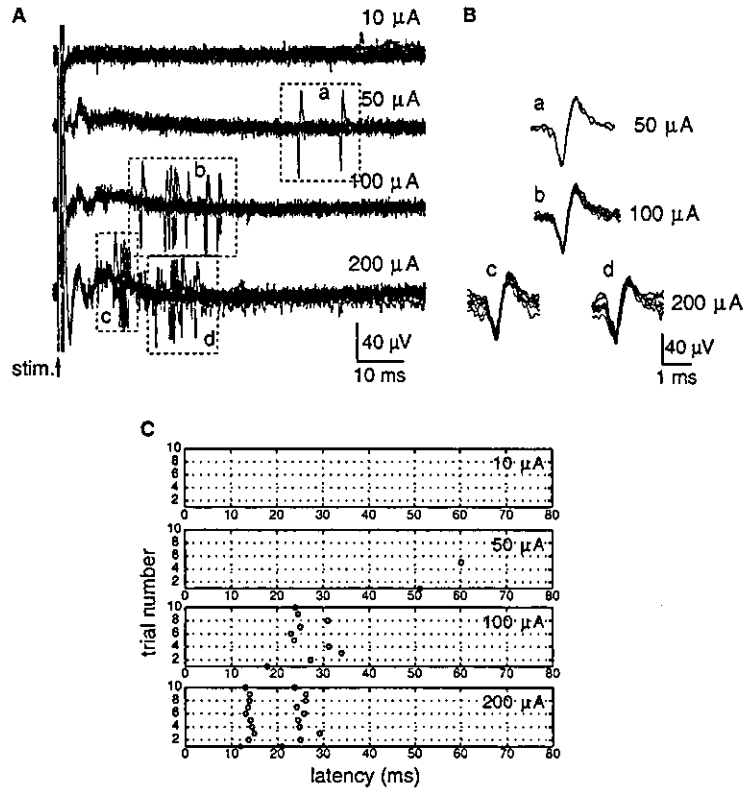

Fig. 4. Effect of stimulus amplitude on responses with a variable latency. The distance between the stimulation and the recording sites was 960 μm. (A) The pulse and the inter-pulse durations of stimuli were fixed at 500 and 100 μs, respectively. Each trace is the superposition of recordings of 10 trials. The arrow labeled "stim" represents the onset of the current stimulus. No response with a constant and short latency was observed in these recordings. (B) The superimposed spikes in expanded scale. The spikes were re-plotted from the responses in (A). (C) Raster plots showing the spike timings measured at different amplitudes of stimulus.

a latency of 65.5 ms (indicated by an arrow) appeared after the first spike that had a similar latency to the other nine trials. The latency of the single spike in 9 trials and the first spike in sixth trial was 27.4 ± 4.2 ms (10 trials). The latencies of the spikes became shorter and the second spike was seen in each trial when the pulse duration of stimulus was further increased to 1000 μs. The latency of the first spike was 15.2 ± 0.8 ms (10 trials) and that of the second one was 28.8 ± 2.6 ms (10 trials) in this case.

The effects of the inter-pulse duration on responses with a variable latency were investigated (15 cells in 6 retinas). Fig. 6 A shows the superimposed responses induced by different inter-pulse durations. B shows raster plots of the spikes recorded in 10 trials. As shown in the figure, no obvious spike was recorded when there was no inter-pulse duration in the stimulus. A spike was elicited in 2 out of 10 trials when the inter-pulse duration was increased to 100 μs. As the inter-pulse duration was increased further to 500 μs, a single spike was induced in 9 trials and two spikes in the first trial. The latency of the single spike in 9 trials and the first spike in the first trial was 30.1 ± 6.0 ms (10 trials). Further increase of the inter-pulse duration to 1000 μs did not alter response latency significantly (30.7 ± 6.0 ms, 10 trials).

In Fig. 6C, the shortest inter-pulse duration of the stimulus to induce the response is plotted as a function of the charge applied per phase for 9 cells examined. As will be shown in the next section, the threshold of excitation can be evaluated in terms of the charge per phase of the current stimuli within a range used in the present study, when the inter-pulse duration was fixed. As shown in the figure, the shortest inter-pulse duration to induce the response decreased as the applied charge was increased. This suggests that the second negative pulse of the stimulus has a suppressive effect on the excitation induced by the first positive pulse.

3.2.3. Charge dependence of the response

In the previous sections, the effects of the stimulus amplitude and pulse duration on the induced responses were examined. The threshold and the number of spikes were highly dependent not only on the amplitude but also on the duration of stimulus in the response with a variable latency. It has been reported in previous exper-

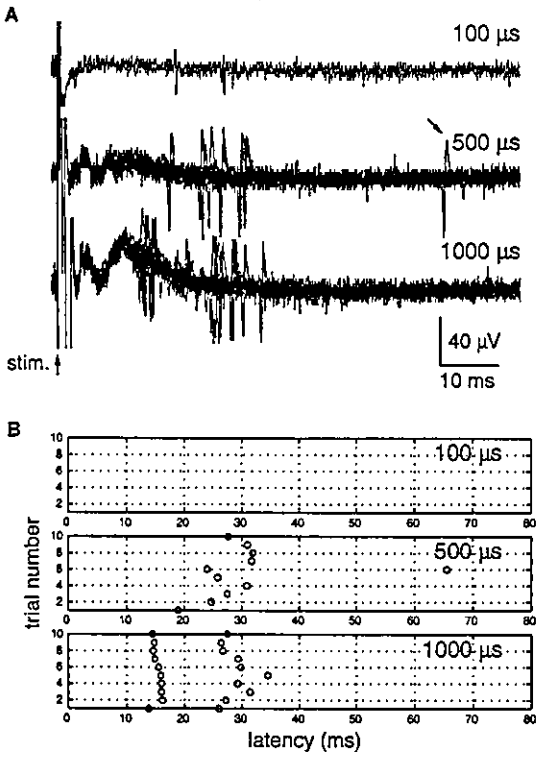

Fig. 5. Effect of stimulus pulse duration on responses with a variable latency. The recordings were obtained from the same ganglion cell as in Fig. 4. (A) The amplitude and the inter-pulse duration of stimuli were fixed at 100 µA and 100 µs, respectively. Each trace is the superposition of recordings of 10 trials. The arrow labeled "stim" represents the onset of the current stimulus. No response with a constant and short latency was observed in these recordings. (B) Raster plots of the spikes induced with different stimulus pulse durations.

iments that the effect of electrical stimuli delivered with a monopolar electrode can be evaluated by the total charge of the stimulus. Namely, the electrical stimuli from the monopolar electrode give rise to similar response properties when measured with the total charge applied (Humayun, 2001).

Fig. 7 shows the responses to stimuli having an equal charge per phase, which is calculated by multiplying the amplitude by the duration of the first positive pulse, but different amplitude and pulse duration. The responses shown in A were recorded when the charge per phase was 50 nC. The upper trace in A shows the response to the stimulus, the amplitude and the pulse duration of which was 100 µA and 500 µs, respectively. The lower trace shows the response to the stimulus with amplitude and pulse duration of 200 µA and 250 µs, respectively. The timing of the spike induced by each stimulus is shown in C. The spike latency of the upper trace of A was 28.5 ± 4.8 ms (10 trials), and that of the lower trace of A was 31.4 ± 5.4 ms (7 trials). B shows responses obtained when the charge per phase was increased to 100 nC. In this case, the stimulus used in the upper trace

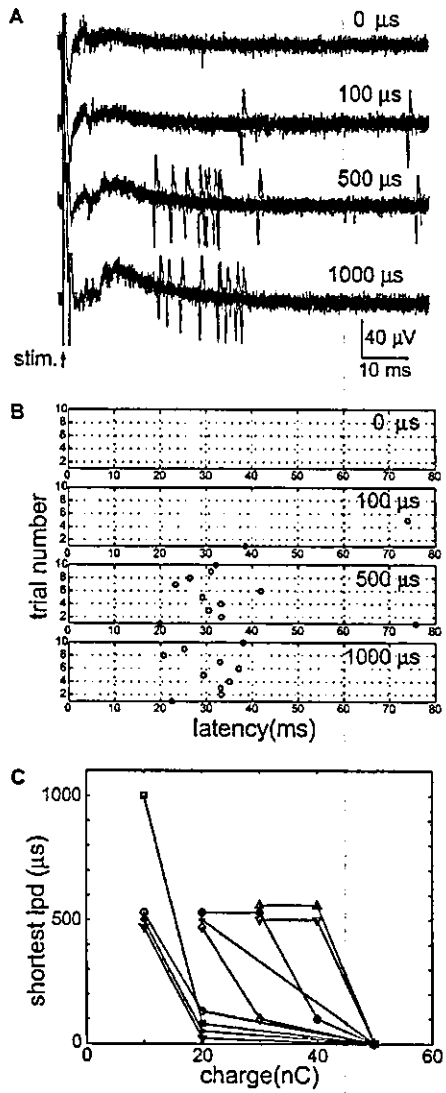

Fig. 6. Effect of stimulus inter-pulse duration on responses with a variable latency. The recordings were obtained from the same ganglion cell as in Fig. 4. (A) The amplitude and the pulse duration of stimuli were fixed at 200 µA and 200 µs, respectively. The total charge applied per phase of the stimulus was 40 nC. Each trace is the superposition of recordings of 10 trials. The arrow labeled "stim" represents the onset of the current stimulus. No response with a constant and short latency was observed in these recordings. (B) Raster plots of the spikes induced with different stimulus inter-pulse durations. (C) The shortest inter-pulse duration of stimulus to induce the response is plotted as a function of the charge (per phase) applied with the stimulus. Each symbol represents a different cell. Each point was slightly shifted along the vertical axis to avoid overlaps. Data from nine cells were plotted in the figure. The shortest inter-pulse duration to induce responses decreased as the charge was increased.

had amplitude and pulse duration of 200 µA and 500 µs, respectively, and that used in the lower trace had amplitude and pulse duration of 100 µA and 1000 µs, respectively. The timing of the spike induced by each stimulus is shown in D. The latency of the first spike